CHAPTER 13

HISTORY OF THE PACIFIC SUPERPLUME: IMPLICATIONS FOR PACIFIC PALEOGEOGRAPHY SINCE THE LATE PROTEROZOIC

ATSUSHI UTSUNOMIYA[1,2,4], TSUTOMU OTA[1,5], BRIAN F. WINDLEY[3], NORIHITO SUZUKI[1], YUKO UCHIO[1,6], KUNIKO MUNEKATA[1], AND SHIGENORI MARUYAMA[1]

[1] *Department of Earth and Planetary Sciences, Tokyo Institute of Technology, O-okayama 2-12-1, Meguro, Tokyo 152-8551, Japan*

[2] *Interactive Research Center of Science, Tokyo Institute of Technology, O-okayama 2-12-1, Meguro, Tokyo 152-8551, Japan*

[3] *Department of Geology, University of Leicester, Leicester LE1 7RH, UK*

[4] *Now at Institute of Earth Sciences, Academia Sinica, Nankang, Taipei 11529, Taiwan; E-mail: uchii@earth.sinica.edu.tw*

[5] *Now at Institute of Study of the Earth's Interior, Okayama University, Misasa, Tottori 682-0193, Japan*

[6] *Now at Public Relations Department, Public Relations Division, National Science Museum, Taito, Tokyo 110-8718, Japan*

Abstract

We have reconstructed the paleogeography of continents, oceans and oceanic large igneous provinces (LIPs) since 1000 Ma in order to decode the history of the Pacific Superplume, using the most reliable recent data for accretional geology from orogens associated with ophiolites and greenstone belts, and of geochronologic and paleomagnetic data from each continent. From our reconstructions we have arrived at the following conclusions: (1) the Pacific Superplume was born at 750 Ma and broke-up the supercontinent Rodinia; (2) the African Superplume was born at 200 Ma and broke-up Pangea; (3) the Pacific Superplume was active episodically with culminations at 580–600 Ma, 280–230 Ma and 150–75 Ma; (4) during the formation of Rodinia much oceanic lithosphere from the Tethyan-Indian type ocean was subducted along paleo-trenches of proto-Grenville orogens along a V-shaped, double-sided convergent boundary around the continental lithosphere of Rodinia. These relations suggest that the massive volumes of lithosphere subducted under the Pacific-type orogens triggered the birth of the Pacific Superplume after 200 m.y. at the center of Rodinia.

D. A. Yuen et al. (eds.), Superplumes, 363–408.
© 2007 *Springer.*

1 INTRODUCTION

A super-upwell in the mantle, i.e., "superplume", was first invoked in the early stages of seismic tomography (Dziewonski, 1984; Woodhouse and Dziewonski, 1984; Dziewonski and Woodhouse, 1987). This revealed two low-velocity domains of seismic waves extending continuously between the uppermost and lowermost mantle, originating under the South Pacific and Africa. These major cylindrical structures with a girth extending for ca. 1000 km are much wider than a skimpy jet plume that gives rise to a so-called hot spot on the Earth's surface. Since the early 1990's, the heterogeneity of the velocities in the mantle has been well defined by seismic tomography with a higher resolution than before (e.g., Fukao, 1992). The lower velocity area in the lower mantle is considered to be a superplume that is a huge mantle plume rising from the core-mantle boundary (CMB), and the higher velocity area at ca. 670 km depth is regarded as a megalith that is interpreted as a massive stagnant slab. These images illustrate the process of 'plume tectonics' (Maruyama, 1994). Although plate tectonics only treats the uppermost 100 km of the solid Earth, whole Earth dynamics includes plate tectonics and plume tectonics which is controlled by episodic superplume activities. Whole Earth dynamics operates at three levels: (1) the subsurface domain is controlled by plate tectonics; (2) the lower mantle is controlled by plume tectonics; and (3) growth tectonics takes place in the core. Plate tectonics puts cold slabs into the mantle. A cold slab stagnates at the mantle transition zone for 100–400 m.y., subsequently collapses, and falls to the surface of the outer core; this results in episodic super-downwelling in the whole mantle and a new downflow in the core. A counter flow to the super-downwelling is the super-upwelling of the hot mantle that causes continental break-up, subsequent dispersal, and formation of large igneous provinces (LIPs) that include flood basalts and oceanic plateaus. Fragmented continents collide and amalgamate to form new large composite continents. During such a process a subducting slab descends to the mantle through trenches around a new continent, and this leads to the next super-downwelling beneath the continent.

Seismic tomography only provides a static image of present superplume activity. From the viewpoint of plume tectonics, the history of supercontinents and LIPs is closely related to the superplume activity. In other words, we can draw essential, although indirect, information about the history of a superplume by decoding the geological records of supercontinents and LIPs that remain on the surface of the Earth. The distribution of ancient continents and orogens preserves a record of where oceanic lithosphere subducted and slabs stagnated. The distribution of LIPs represents where mantle upwelling occurred. Furthermore, ophiolites and greenstone belts provide information on the oceanic domains of LIPs and on oceanic lithosphere that disappeared into the mantle.

In this paper, in order to understand the activity of the Pacific Superplume, we discuss the paleogeographic reconstruction of continents and oceans since 750 Ma from an evaluation of the most recent reliable data on regional geology, geochronology and paleomagnetism from each continent. Our reconstruction concerns not only the

distribution of continents, but also of mid-oceanic ridges and trenches. In addition, ancient LIPs, which occur in oceanic regions or are partly trapped in current orogens, are reconstructed with data from accretionary geology. Comparing the Pacific and African Superplumes, we have decoded the general modes of interaction between plume activity and plate tectonics in the Earth's late history.

2 METHODS AND DATA SOURCES FOR RECONSTRUCTION

2.1 Continental reconstructions

Since the development of plate tectonics in the 1970's, numerous paleogeographic maps have been published. In particular, the Paleogeographic Atlas Project (University of Chicago, http://pgap.uchicago.edu/PGAPhome.html), the PLATES project (University of Texas at Austin, http://www.ig.utexas.edu/research/projects/plates/) and the PALEOMAP project (University of Texas at Arlington, http://www.scotese.com) have produced systematic series of paleogeographic maps for several decades. For their constructions they integrated vast amounts of data from paleomagnetism, sea floor linear magnetic anomalies, paleogeography, paleoclimatology and geology. Although the Paleogeographic Atlas Project concentrated on the Mesozoic and Cenozoic, the PLATES and PALEOMAP projects extended from 750 Ma to the present. Although they have reached a general consensus on Cenozoic and Mesozoic continental distributions, their Paleozoic and Neoproterozoic reconstructions are significantly different. Our maps of continental distributions are mainly dependent on the latest paleogeographic maps of the PALEOMAP project (Scotese, 2004). The contributions of individual paleomagnetists and their groups will be referred to specifically in the text.

Figure 1 is a compilation map showing the worldwide distribution of geologic units in continents and oceans of different ages based on published data, in particularly from Liou et al. (1990), Windley (1995), and Maruyama et al. (1996), and references therein. A general view of the compiled map shows that most continents are composed of Precambrian nuclei (cratons) and orogenic belts with zonal growth toward their exteriors. Two types of orogens form at convergent plate boundaries. Collisional orogens result from continent-continent collisions and may involve some arc accretion, and Pacific-type orogens develop as a result of oceanic plate subduction and accretion (e.g., Maruyama, 1997). The temporal and spatial distribution of collisional orogens provides data on the timing of continental amalgamation, and that of Pacific-type orogens supplies direct information on the distribution of trenches. Surely orogenic belts cannot be developed from continental rifts. Only rifts are developed from rifts. A rifting event is accompanied by large-scale magmatism. Their traces of which are preserved as dyke swarms remain on drifted continental margins. At the initial stage of continental rifting, extensive dike swarms are intruded perpendicular to the rift axes, as best documented along the Mesozoic coast lines in the Atlantic Ocean (Ruffman and Greenough, 1990; Hill, 1991). The intrusion ages and distribution of the dykes provide essential information on continental breakup.

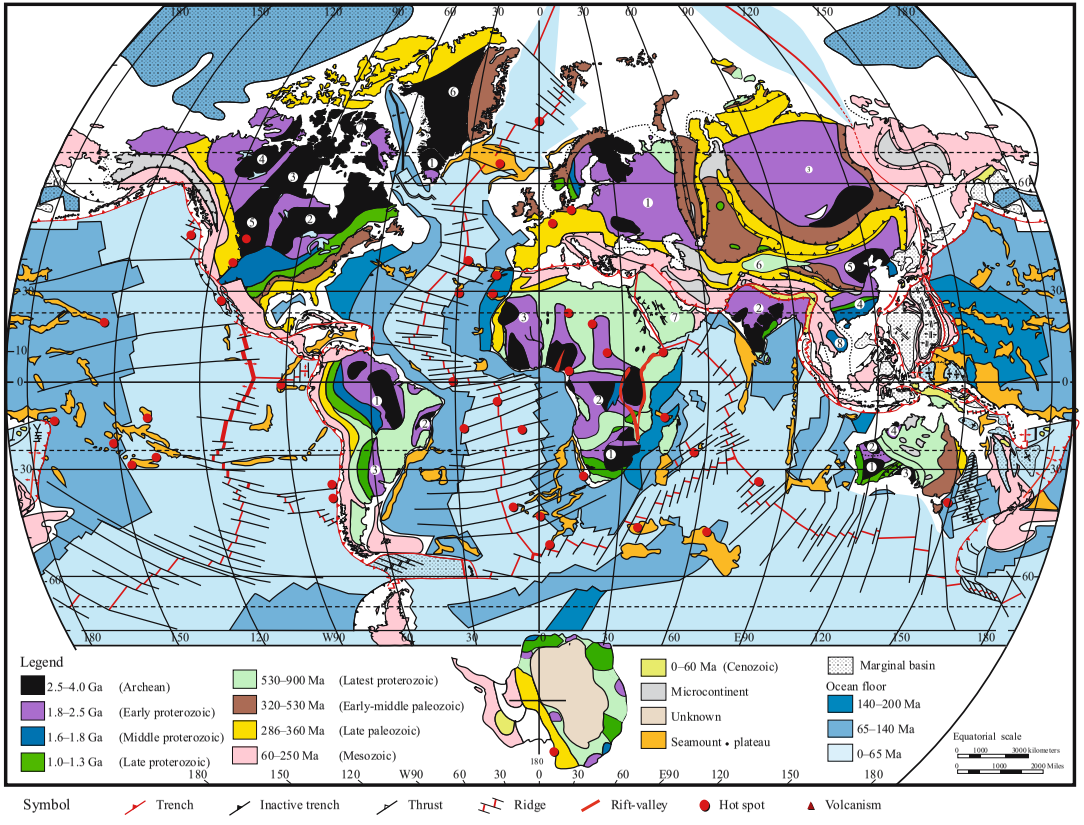


Figure 1. Compilation map of orogenic belts worldwide. Major cratons in each continent are numbered: (Asia-Europe) 1 = Baltica craton; 2 = Indian craton; 3 = Siberian craton; 4 = South China craton; 5 = North China craton; 6 = Tarim block; 7 = Arabian shield; 8 = Indochina block; (Australia) 1 = Yilgarn; 2 = Pilbara; 3 = Gawaler; 4 = Kimberley; (North America) 1 = Nain; 2 = Superior; 3 = Hearne; 4 = Slave; 5 = Wyoming; 6 = Nagssugtoqidian; 7 = Rae; (South America) 1 = Amazonia; 2 = Sao Francisco; 3 = Rio de La Plata; (Africa) 1 = Kalahari; 2 = Congo; 3 = West Africa.

We assessed the maps of the PALEOMAP project by utilizing reliable recent data from continental collisional orogens and correcting them if inconsistent. We decoded the distributions of trenches from Pacific-type orogens and superimposed them on the maps.

2.2 Paleogeographic reconstructions of oceanic domains

The existence of magnetic stripes on the oceanic floor, the distribution of fracture zones, and the assumption that hotspots in the Pacific and Atlantic Oceans are mutually fixed, provided information for the relative motions between the major plates and the distribution of mid-ocean ridges and trenches in the Pacific Ocean (e.g., Engebretson et al., 1985). The paleopositions of oceanic plateaus dispersed in the Pacific Ocean were reconstructed by using the relative motions model (Larson, 1991a). These reconstructions are available only for the last 140 Ma, because most of the older oceanic crust has disappeared into the mantle at subduction zones. But a few fragments of the old oceanic plates remain in the Pacific-type orogens. These fragments occur as on-land ophiolites/greenstone belts (Fig. 2). In this study, we extracted information

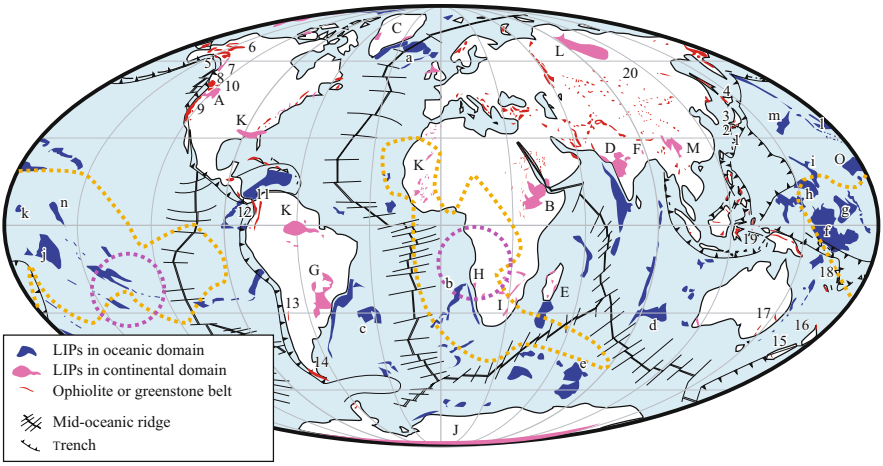


Figure 2. Distribution map of LIPs, ophiolites and greenstone belts over the world (after Coffin and Eldholm, 1994; Mann and Taira, 2004). The regions enveloped by orange and purple dashed lines show the seismic lower velocity zones (Vs) at 2850 m depth in lower mantle and superswell regions, respectively (Courtillot et al., 2003). These express the present superplume roots and active areas. Numbers of ophiolites and greenstone belts listed in Table 2. A = Columbia River basalts; B = Ethiopian and Yemen Traps C = NAVP; D = Deccan Trap; E = Madagascar basalts; F = Rajmahal basalts; *G* = Paraná basalts H = Etendeka basalts; I = Karoo basalts; J = Ferrar basalts; K = CAMP; L = Siberian Trap; M = Emeishan flood basalts. a = Iceland; b = Walvis Ridge; c = Rio Grande plateau; d = Broken Ridge; e = Kerguelen Plateau; f = Ontong Java plateau; g = Nauru Basin; h = East Mariana Basin; i = Pigafetta Basin; j = Manihiki Plateau; k = Magellan Rise; l = Hess Rise; m = Shatsky Rise; n = Line Islands; o = Mid-Pacific Mountains.

on the oceanic domains from the Pacific-type orogens and reconstructed the paleogeography of oceanic domains that included the distribution of mid-ocean ridges, oceanic islands, and oceanic plateaus.

2.2.1 Extraction of oceanic information from pacific-type orogens

Accretionary geology. Compilation of the Pacific-type orogens enabled us to reconstruct the paleo-positions of trenches. Moreover, an accretionary complex in a Pacific-type orogen is a repository of information on oceanic regions, because it captures material from an oceanic plate subducting through a trench. The geologic structure of an accretionary complex is characterized by duplexes (Fig. 3). A duplex has an internal structure in which each faulted-package (horse) is subparallel or oblique to a roof or floor thrust and each duplex is separated by a link thrust. Each horse in the duplex preserves primary stratigraphic relations of oceanic rocks (basal basalt, pelagic bedded chert or micritic limestone, hemipelagic siliceous mudstone or shale capped by trench-fill terrigenous turbidite. This complex structure was unraveled by microfossil mapping (Matsuda and Isozaki, 1991). The ages of the constituents in the

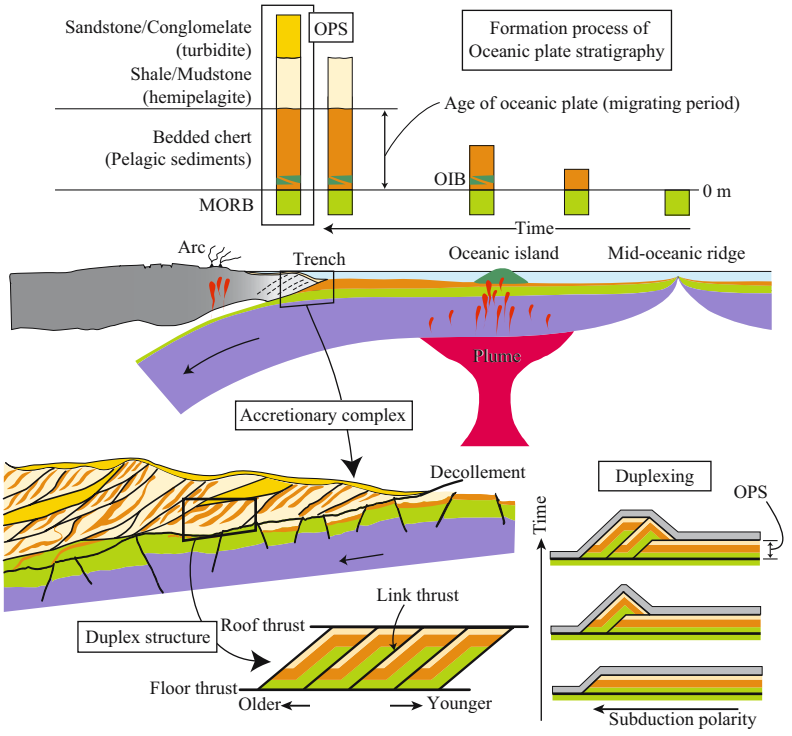


Figure 3. Formation process of oceanic plate stratigraphy and an accretionary complex. See text for explanations.

horses of a particular duplex become younger oceanward, because of their oceanward growth with time: moreover, the duplex develops downward with time. Such primary stratigraphy in an accretionary complex is called "ocean plate stratigraphy" (OPS); it preserves the stratigraphic relations of the rocks and strata of the upper oceanic plate as it moves from ridge to trench. Where the oceanic rocks are covered conformably with terrigenous clastic sediment, the age of that clastic horizon approximates the time of formation of the accretionary complex at the trench. And, accordingly the deposition time of the oceanic sediments is the time interval between the lowermost and uppermost beds of the pelagic and hemi-pelagic sediments, i.e., it indicates the length of time it took for the oceanic plate to move from the mid-oceanic ridge to the trench. That is to say, the deposition time interval of the oceanic sediments is the age of the oceanic plate, which subducts at the trench. Consequently, OPS, which is now exposed on land, provides us with information on how old the oceanic plate is, and when it entered the accretionary complex. The best high-precision method to determine these ages is microfossil dating with radiolarian stratigraphy in the pelagic and terrigenous sediments in Phanerozoic strata (Isozaki et al., 1990; Matsuda and Isozaki, 1991). The reliable Ar-Ar dating is also available to determine the eruption age. In the case of Proterozoic OPS, in which it is difficult to obtain microfossils, the best methods are U-Pb and Pb-Pb dating of heavy minerals such as zircon and a bulk isochron.

Summary of modern volcanic sequences. Information about oceanic materials, i.e., basaltic greenstones and associated sedimentary rocks, in accretionary complexes, is essential to reconstruct the oceanic paleogeography. In this study, we compared the characteristics of modern volcanic sequences in oceanic domains (Table 1) with those of oceanic materials extracted from accretionary complexes, and so worked out their primary tectonic settings such as mid-ocean ridge, off-ridge (oceanic islands, seamounts and oceanic plateaus), fore-arc or back-arc basin, and island arc.

In terms of the geologic features in modern tectonic settings, shallow-marine pelagic sediments such as limestone are suggestive of deposition on a topographic high in the mid-ocean, whereas thick deep-sea pelagic sediments like bedded chert are characteristic of the mid-ocean floor. Terrigenous sediments are expected to be the predominant lithology in a trench near an island arc, where chert and carbonate can be recognized but distinguished from the mid-oceanic sediments, by their thickness and association with terrigenous materials. In this regard, when a mid-ocean ridge reaches a trench, terrigenous sediment rather than pelagic chert will directly cover the mid-oceanic ridge basalts (MORB).

Other key geologic features of modern volcanic sequences are the modes of occurrence of their crustal constituents. Subaerial eruption is characteristic in oceanic islands and island arcs due to their topographic features, whereas pillow lavas indicate submarine settings, i.e., seamounts, mid-ocean ridges and back- and fore-arc basins. The presence of sheeted dykes is conclusive evidence of a spreading center like a mid-ocean ridge. As for the crustal thickness of volcanic sequences (above the Moho depth), there is a distinct contrast between oceanic plateaus and other environment.

Table 1. Geological and petrochemical characteristics of volcanic sequences from different tectonic setting

Tectonic setting	Oceanic plateau (OP)	Oceanic island/seamount (OI/SM)		Mid-ocean ridge (MOR)	Marginal basin (MB; back-/fore-arc basin)	Island arc (IA)
Predominating sediments	Shallow-marine pelagite	Shallow-marine pelagite		Deep-sea pelagite	Hemipelagite, terrigenous clastics	Terrigenous clastics
Crustal thickness	20–40 km	7–15/7–10 km		<7 km	<7 km	7–20 km
Ocean floor metamorphism (gabbro layer)	Granulite facies	Amphibolite facies		Amphibolite facies	Amphibolite facies	Granulite facies
Dyke complex	Not sheeted	Not sheeted		Sheeted	Sheeted	No
Texture of volcanics	Mainly aphyric	Porphyritic		Mainly aphyric	Mainly aphyric	Porphrytic
Fractional control	Ol, Cpx, Pl	Ol, Cpx		Ol, Pl	Ol, Cpx, Pl	Ol, Opx, (Cpx), Amp
Type of basalt	TH, A	A, TH		TH	TH, A	CA, TH, A
(La/Nb)n	≤1	≤1		≤1	from ≤1 to >1	≫1
REE pattern	Mainly flat	LREE enriched + HREE depleted		LREE depleted	Mainly flat	LREE enriched
		Normal hotspot	Superplume-related			
Nb/Y		<5.5(Nb/Zr) + 0.5	>5.5(Nb/Zr) + 0.5			
			Non-HIMU HIMU			
Nb/Zr			<0.23 >0.23			
$^{206}Pb/^{204}Pb$			<20.5 >20.5			

Ol, olivine; Cpx, clinopyroxene; Opx, orthopyroxene; Pl, plagioclase; Amp, amphibole; TH, tholeiite; A, alkaline rock; CA, calc-alkaline rock.

For example, the Ontong Java plateau has an average crustal thickness of about 33 km (e.g., Richardson et al., 2000), and other oceanic plateaus have unusually thick crusts. Based on experimental studies, basaltic rocks with a bulk composition of quartz tholeiite or alkali olivine basalt can be transformed to garnet-bearing granulite at c. 1000°C above 1.2 GPa or 0.8 GPa, respectively (e.g., Ringwood, 1975). The unusual thickness of an oceanic plateau would cause metamorphism at the base of the plateau crust at higher pressure and temperature conditions than at a normal mid-oceanic ridge. The crustal thickness of oceanic plateau could form garnet-bearing granulites like mafic xenoliths found from the northern end of the Kerguelen plateau (Gregoire et al., 1994), although it depends on the availability of fluids and chemical compositions of lower crusts of the plateau. In contrast, the thickness of common oceanic crust does not usually exceed c. 7 km, and the confirmed maximum grade of modern ocean-floor metamorphism is in the amphibolite-facies, except for a very rare case in the Mid Atlantic Ridge (e.g., summary in Ishizuka and Suzuki, 1995). In consequence, the mechanism and process "oceanic plateau metamorphism", mentioned above, differs from those of ocean-floor metamorphism in association with hydrothermal alteration at a mid-ocean ridge.

The petrography and petrology of volcanic rocks also vary in different tectonic settings, depending on the rock type and formation process. Oceanic island basalts (OIB) and island arc basalts (IAB) are porphyritic, whereas oceanic basalts in the other settings are mainly aphyric. The fractionation control of plagioclase following olivine is characteristic in MORB consisting predominantly of low-K tholeiites, whereas OIB are predominantly alkaline rocks and have the crystallization sequence of clinopyroxene following olivine. The crystallization of orthopyroxene and amphibole is a specific feature of IAB associated predominantly with calc-alkaline rocks. However, immature oceanic island arc basalts are predominantly tholeiitic, occasionally associated with boninites and fore- and back-arc-basin basalts, and are similar to MORB. In recent years, it has been established that oceanic plateau basalts (OPB) are generally aphyric and their fractionation is controlled by olivine, plagiolclase and clinopyroxene, depending on the depth of their generation (e.g., Neal et al., 1997), whereas the fractionation of MORB is generally controlled by olivine and plagioclase.

The geochemical characteristics of basaltic rocks can be used to distinguish their parental materials and formation processes. Chondrite-normalized rare earth elements (REE) patterns with depletion of light-rare-earth elements (LREE) are typical of normal-type (N-) MORB (e.g., Sun and McDonough, 1989). OIB have a REE pattern with high LREE-enrichment and the depletion of heavy-rare-earth elements (HREE). Depletion of high-field-strength elements (HFSE) relative to large-ion-lithophile elements (LILE), and distinctive Nb anomalous behaviors in primitive mantle-normalized incompatible elements patterns, are suggestive of calc-alkaline IAB, the sources of which are affected by subduction-zone metasomatism; this is termed a suprasubduction characteristic. Back- and fore-arc-basin basalts have transitional signatures between IAB and N-MORB with relative Nb depletion. Immature oceanic island arc tholeiites also have a negative Nb anomaly. OPB have a flat REE pattern similar to enriched-type (E-) MORB.

Radiogenic isotopic compositions of basalts are a powerful tracer to determine their source materials, because they have not involved a fractionated magmatic process, such as partial melting or fractional crystallization. MORB have depleted components (DM), and OIB have enriched components (EM1, EM2, and HIMU; e.g., Zindler and Hart, 1986). HIMU basalts, which are enriched in radiogenic Pb ($^{206}Pb/^{204}Pb > 20.5$), are restricted to superplume regions (Cook-Austral, Polynesia; St. Helena). OPB have an OIB-like radiogenic isotopic signature.

Criteria for discrimination of tectonic settings of ancient volcanic sequences in accretionary complexes. As described above, modern volcanic sequences have different geologic, petrochemical and isotopic features according to their tectonic settings. Therefore, these features in ancient volcanic sequences trapped in accretionary complexes can help us distinguish their tectonic settings.

In terms of geologic features, sedimentary rocks such as limestone, bedded chert and terrigenous clastics associated with basaltic greenstones in accretionary complexes, and their mutual structural relationships (e.g., conformable or not) provide us with useful information to reconstruct the environment where the greenstones were erupted. When an oceanic plate is trapped in an orogenic belt, rocks from various depths of the plate may be exposed after their uplift and erosion. Metamorphic petrology of such rocks, i.e., the degree of ocean floor metamorphism, enables us to reconstruct their primary geologic structure and original tectonic setting; if there is any evidence of high-pressure granulite-facies ocean floor metamorphism, this must be derived from the lower crust of an oceanic plateau.

The geochemical and isotopic features of modern basaltic rocks from various tectonic settings can be distinguished by several discrimination diagrams (e.g., summary in Wilson, 1989; Rollinson, 1993). However, these discrimination diagrams may not always lead us to confident conclusions for determining the tectonic settings of greenstones. Discrimination diagrams based on compilations of published data only suggest the general petrogenesis of the greenstones, and do not indicate directly their tectonic settings. Moreover, greenstones trapped in orogenic belts have been subjected to secondary modification by hydrothermal alteration and metamorphism during their travel to a trench, after their travel from their birth place. LILE are highly mobile under these processes, and so their contents in greenstones cannot be used to determine their tectonic setting. For the same reason, although the Pb isotopic ratio of HIMU basalts is a conclusive characteristic for distinguishing its origin, Sr and Pb isotopic compositions are easily modified by hydrothermal alteration. But, HFSE such as Nb, Y and Zr, and REEs are generally regarded as immobile against secondary alteration, and the systematics of these elements are useful for discrimination of greenstones. Nd isotope compositions are also available as a discriminant. Tatsumi et al. (1998) pointed out that superplume-related OIB have higher Nb/Y ratios than other OIB at given Nb/Zr ratios, and in particular HIMU basalts have higher Nb/Zr ratios. If Pb isotopic compositions are not available, we can indirectly trace superplume-related volcanism using Nb-Zr-Y systematics that resist alteration.

Cretaceous oceanic plateaus, dispersed at present in the southwestern and western Pacific, formed in the Pacific Superplume region (e.g., Larson, 1991a). However, most basalts from those oceanic plateaus show tholeiite-like geochemical characteristics similar to E-MORB, and are homogeneous in composition (e.g., Mahoney et al., 1993), except for some alkaline basalts with the HIMU signature (Tejada et al., 1996). Therefore, these tholeiitic OPB exhibit different trends on a Nb/Y-Nb/Zr diagram (Tatsumi et al., 1998) from the superplume-related OIB. Such a difference could be caused by the formation process of such a huge amount of plateau basalt; melting a large amount of lithospheric mantle could dilute the geochemical signature of the HIMU end-member in the resultant melt. Except for well analyzed cases (the Solomon islands and the Ontong Java plateau), the petrochemical characteristics of oceanic plateau basalts have been studied by using restricted samples dredged from the ocean floor that provide only limited information on the subsurface of the oceanic plateaus. Because of these problems, it is controversial whether superplume-related plateau basalts can be definitely characterized only by geochemical characteristics such as the HIMU signature and Nb-Y-Zr systematics. So, we must pay attention to other aspects of oceanic plateaus or OPB, i.e., their geologic, petrographic and petrologic features such as crustal thickness, type of phenocrysts, compositional trend by differentiation, and so on (Table 1).

As stated above, a comprehensive examination enables determination of the tectonic settings of greenstones in orogenic belts. With such considerations, we determined the primary tectonic settings of ophiolites and accreted greenstones in orogenic belts mainly in the circum-Pacific region, listed in Table 2. The compilations for the study were taken from the most recent and reliable data available at present, since the quality and quantity of available data are uneven according to area and age.

2.2.2 Procedures of reconstruction of oceanic domains

Cenozoic-mesozoic reconstruction. The distribution of mid-ocean ridges and trenches for the last 200 Ma is well known and plate reconstructions are available, because information on the oceanic domain is immediately retrievable from the extant oceanic floor.

As stated above, the paleopositions of the Cretaceous LIPs in the present oceanic domain can be estimated by using the relative plate motions model (Engebretson et al., 1985; Larson, 1991a); those oceanic LIPs were put back from the present day to their erupted age, following their plate motions. For the ophiolites and greenstones in accretionary complexes of the Pacific-type orogenic belts, at first we distinguished their tectonic settings on the basis of the above-mentioned criteria and available data about their geology, geochronology and petrochemistry. After that, the paleopositions of the ophiolites and greenstones were reconstructed using the relative plate motion model (Engebretson et al., 1985). In a case where a determined setting was an island arc, back- or fore-arc basin, the ophiolites or greenstone belts were generated at a continental margin at that period, and migrated with it until the present. In the case of oceanic settings, we determined the formation age from microfossils from the bottom of the sedimentary section of the OPS, from trapped sediments in lavas,

Table 2. Summary of circum-Pacific ophiolities and greenstone belts

No.	Name	Region	Type	Eruption age	Accretion age, Ma
5	Resurection peninsula and knight island ophiolites (Orca group)	N. America	MOR (TTR)	57 Ma	
1	Melange in shimanto supergroup	E. Asia	MOR (TTR)	Cenomian-earliest paleocene	
18	New caledonia ophiolotite	Oceania	MB, OI, IA	Campanian-upper paleogene, upper paleocene (56–59 Ma)	
16	Tangihua ophiolite (Northland ophiolite)	Oceania	MB	mod-creataceous-paleocene	
11	Caribbean plateau	C. & S. America and Caribbean Sea	OP	90 Ma, 75 Ma	Late cretaceous (85–83 Ma)
12	Gorgona plateau	S. America	OP	90 Ma, 75 Ma	Late Eocene
19	East sulawesi ophiolite		OP	138 Ma	>28 Ma
2	Iratsu massif (Sanbagawa belt)	E. Asia	OP	142–153 Ma	110–120 Ma
4	Sorachi-yezo belt	E. Asia	OP	150 Ma	Barremian
8	Josephine ophiolite	N. America	MB	157 Ma	151 Ma
9	Coast range ophiolite	N. America	IA, SM	160–170 Ma	
7	Wrangellia terrane	N. America	FB	middle ladonian-late karmian	
14	Aysen metamorphic complex	S. America	OP, OI (superplume)	Late triassic, Late devonian	
3	Yakuno ophiolite	E. Asia	OP	282–285 Ma	
6	Angayucham terrane	N. America	OP	Mississipian	Middle jurassic
15	Dun mountain ophiolite	Oceania	MA	280 Ma	
17	Tasmanide ophiolite	Oceania	IA	514 Ma, 524 Ma, 503 Ma, 502 Ma, 530 Ma, 509 Ma, 535 Ma	
10	Trinity ophiolite	N. America	IA-MB	565–570 Ma, 452 Ma, 412 Ma	
13	Precordillera ophiolite	S. America	OP	576 Ma	
20	Kurai greenstone	C. Asia	OP	598 Ma	

or directly from the isotopic age of the volcanics. In a similar way, we determined the emplacement age on the basis of microfossils from the terrigenous horizon of the OPS. From the present day to their emplacement age, we considred that they were considered to have migrated with their relevant continents, whereas from their emplacement age to eruption age, the same method for the LIPs in the present oceanic domain was adopted.

Paleozoic-neoproterozoic reconstruction. Location of mid-oceanic ridges were considered in terms of a model in which the mid-oceanic ridges were present at the center of a small ocean surrounded by continental fragments for the period from continental break-up to initiation of plate subduction. After the beginning of subduction, the locations of mid-oceanic ridges are unknown because we have no method of deciding the relative velocity between the oceanic plates. In such cases, we tentatively arranged the mid-oceanic ridges anywhere in the oceans.

The ophiolites and greenstone belts in accretionary complexes were examined for their tectonic setting based on the criteria mentioned above. In cases where they were generated at a continental margin, they could migrate with the continents. In the case of an oceanic setting, we could not directly use the plate motions. If paleomagnetic data were available, we were able to use them. But in most cases, they were not available and we could not determine their detailed positions in the ocean. We could only determine the pelagic environment in an ocean that faces an orogenic belt. In cases where greenstones or ophiolites had superplume affinities or oceanic plateau affinities and the orogenic belts faced the Pacific Ocean, they could be located in the Pacific Superplume region at their eruption age, based on the analogy that Cretaceous oceanic plateaus were generated in the Pacific Superplume region.

3 RECONSTRUCTIONS

3.1 From 200 Ma to the present

3.1.1 Continental domain

In this period, the history of continents involved the breakup of the supercontinent Pangea and the redistribution of the fragments (e.g., Ford and Golonka, 2003; Golonka et al., 2003, and references therein). Rifting of Pangea was initiated in the Early Triassic. The drift-rift transition occurred at ∼200 and ∼185 Ma in the southeastern US and maritime Canada, respectively. The start of seafloor spreading in the central Atlantic is dated as 175 Ma. The breakup of Africa from India/Antarctica took place in the period 198–173 Ma. The initial opening of South Atlantic between Africa and South America was at 130 Ma. The Central Atlantic Ocean propagated towards the North Atlantic and the onset of seafloor spreading of Rockall Trough started at ∼95 Ma. The separation of Madagascar/India from Africa began at ∼180 Ma and was stable relative to Africa by 112 Ma (Coffin and Rabinowitz, 1988). The breakup of Greater India from Australia is dated as 136 Ma (Müller et al., 1998). The beginning of separation of India from Antarctica and from Madagascar occurred at ∼134 Ma

and at ~88 Ma, respectively (Ramana et al., 2001; Storey et al., 1997). Seafloor spreading at 85 Ma led to the separation of Australia from Antarctica (Norvick and Smith, 2001). The Labrador Sea started to open at 62 Ma (Saunders et al., 1997). South America began to migrate away from Antarctica at ~50 Ma (Livermore et al., 2005).

The extrusion of much continental flood basalt occurred in this period; the Columbia River basalts at 6–17 Ma (Baksi, 1989; Tolan et al., 1989), Ethiopian and Yemen Traps at 30 Ma (Hofmann et al., 1997), North Atlantic Volcanic Province (NAVP) at 60 ± 1 Ma (Eldholm and Grue, 1994), Deccan Traps ~66 Ma (e.g., Baksi, 1994), Madagascar basalt at 88 Ma (Storey et al., 1995), Rajmahal basalt at 116 Ma (Pringle et al., 1994), Paraná-Etendeka basalts at 138–131 Ma (Stewart et al., 1996), Karoo-Ferrar basalts at ~180 Ma (e.g., Marsh et al., 1997), and the Central Atlantic Magmatic Province (CAMP) at 197–201 Ma (Marzoli et al., 1999a,b). The age and distribution of NAVP, the Madagascar, Rajmahal, Paraná-Etendeka and Karoo-Ferrar basalts and the CAMP indicate the initial stage of opening or breakup of the North Atlantic Ocean, Madagascar/India, India/Antarctica, South Atlantic Ocean, Africa/Antarctica, Central Atlantic Ocean, respectively. Except NAVP, these LIPs were generated directly or nearly on the African low seismic velocity area in the lower mantle (Fig. 4). The main breakup event of Pangea occurred in the African Superplume region. Ultramafic lamprophyres in the Ferrar igneous province have a HIMU-signature (Riley et al., 2003), suggesting that breakup of Pangea was controlled by upwelling of the lower mantle.

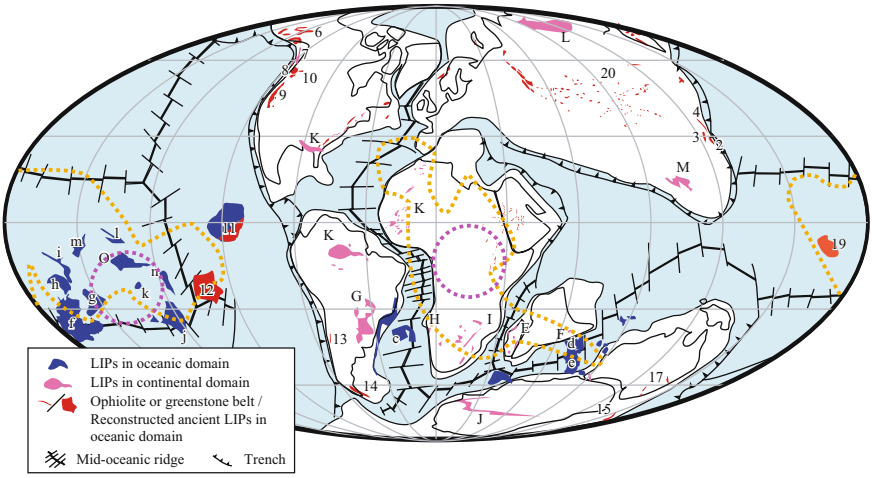


Figure 4. Reconstructed paleogeographic maps at ca. 90 Ma. The distribution of continents is referred to Scotese (2004). Alphabets of LIPs and numbers of ophiolites or greenstone belts are shown as Figure 2. Although Sorachi-Yezo belt (4) and Iratsu massif (2) is generated in superplume region at ca. 150 Ma, they were rapidly transported to subduction zone on Izanagi plate and had already been accreted before 90 Ma.

3.1.2 Oceanic domain

Oceanic plateaus, oceanic floor flood basalts, and aseismic ridges in this period are widely dispersed in the world's oceans. Major examples are: Iceland at 0–15 Ma (McDougall et al., 1984), Walvis Ridge at 79–30 Ma and Rio Grande Plateau at 89 Ma (O'Connor and Duncan, 1990) in the Atlantic Ocean, Broken Ridge at 94–95 Ma, Kerguelen Plateau at 118–34 Ma (Duncan, 2002) in the Indian Ocean, Ontong Java Plateau at 122 and 90 Ma (Mahoney et al., 1993), Nauru Basin at 110.8 Ma (Castillo et al., 1994), East Mariana Basin and Pigafetta Basin at 114.6–126.1 Ma (Pringle, 1992), Manihiki Plateau at 91–114 Ma (Lanphere and Dalrymple, 1976), Magellan Rise at ∼135 Ma (Winterer et al., 1973), Hess Rise at 99–112 Ma (Kroenke and Nemoto, 1982) and Shatsky Rise at 126–150 Ma (Nakanishi et al., 1989) in the Pacific Ocean.

Most oceanic LIPs in the Atlantic and Indian Oceans have a ridge-like geomorphology and a long active time-span, or are related to continental flood basalts by hot spot tracks; e.g., NAVP and Iceland, Paraná-Etendeka basalt and Walvis Ridge-Rio Grande Plateau, and Rajmahal basalt and Kerguelen Plateau-Broken Ridge-Ninetyeast Ridge (Morgan, 1981; Richards et al., 1989). Although some of those in the Pacific have the above-mentioned characteristics, most have short active life spans. Their eruption ages concentrate in the Jurassic-Cretaceous (80–150 Ma) and their paleopositions in the center of the Pacific Superplume region at their generation age (Fig. 4; Larson, 1991a). Furthermore, western Pacific seamounts have non-sequential, synchronous ages and non-concordant chain with the Pacific plate motion (e.g., Line Islands at 81–86 and 68–73 Ma, Davis et al., 2002; Mid-Pacific Mountains at 117–132 Ma, Smoot, 1999), and were derived from the Pacific Superplume along preexisting linear weaknesses in the lithosphere. In this period, the relevant part of the Pacific plate was divided into several micro-plates (Nakanishi and Winterer, 1998) and the Shatsky Rise was generated by propagation of a ridge-ridge-ridge (RRR) triple junction (Nakanishi et al., 1999). These lines of evidence support the idea that mantle upwelling took place.

The Resurrection Peninsula and Knight Island Ophiolites from the Orca Group in southern Alaska contain pillow basalts interbedded with terrigenous sediments and sheeted dykes (Lytwyn et al., 1997). The Resurrection Peninsula Ophiolite is dated as 57 ± 1 Ma by the zircon U-Pb method on intruded plagiogranite. The basalts commonly have plagioclase phenocrysts, clinopyroxene microphenocrysts, and olivine phenocrysts, but have flat REE patterns and transitional-type MORB-like geochemical signatures. These ophiolites were generated at a trench-trench-ridge (TTR) triple junction and are relicts of the subduction of the Kula-Farallon ridge.

Mélange units containing greenstones are common throughout the Shimanto Supergroup in the Ryukyu Islands and southwestern Japan. The greenstones from some formations (Naze Formation, Makimine Formation, Okitsu Mélange, Mugi Formation, Ryujin Formation, and Inui Group) have closely related shales and lack bedded cherts (Kiminami et al., 1994). Radiolarian assemblages from the shales indicate Cenomanian-Turonian, Santonian-Middle Campanian, Coniacian-Campanian, Campanian-Early Maestrichtian, Late Campanian-Maestrichtian, and

Late Maestrichtian-earliest Paleocene ages for the Naze Formation, Makimine Formation, Okitsu Melange, Mugi Formation, Ryujin Formation, and Inui Group, respectively. They all have MORB-like geochemical features, and were generated at a TTR triple junction and are relicts of the subduction of the Kula-Pacific ridge on the basis of these characteristics. The ridge motions by plate reconstructions (Maruyama and Seno, 1986) are consistent with the evidence that the greenstones become younger eastwards (Kiminami et al., 1994).

In New Caledonia in the southwestern Pacific one of the largest ophiolites of the world belongs to the Ophiolitique Nappe, the Poya Terrane and Pouebo Terrane (Cluzel et al., 2001). In the Poya Terrane pillowed and massive basalts, dolerites, and fine-grained gabbros are interbedded with or covered by abyssal argillite and chert. The most common radiolaria extracted from the sedimentary rocks indicate an Upper Cretaceous (Campanian) age. An Upper Paleogene fauna has also been recovered from some localities. Due to the absence of terrigenous materials, it is inferred that the ophiolite was accreted in an intra-oceanic environment. The Poya Terrane in general was metamorphosed in the greenschist facies interpreted as ocean floor metamorphism. However, because the terrane is severely disrupted, the primary thermal structure of the crust cannot be reconstructed. The volcanic rocks from the Poya Terrane are divided into three types on the basis of their REE patterns. An "undepleted type" has a flat REE pattern and contains augite and plagioclase phenocrysts. A "depleted type" has a slightly depleted REE pattern and Nb depletion and contains augite microphenocrysts. Nd isotopic variations of "undepleted" and "depleted" types suggest mixing between DM and EM2 sources. Synthesizing the features above, "undepleted" and "depleted" types are inferred to have been generated in a plume-enhanced marginal basin. The third REE type is an alkaline volcanic rock that has highly enriched REE patterns, is associated with micritic interpillow sediments, and has pinkish Al and Ti-enriched diopside, plagioclase and Fe-Ti oxides microphenocrysts. It is interpreted to have erupted as a seamount in the basin that provided the other types of volcanic rocks. The faunas recovered from micritic interpillowed materials indicate an Upper Paleocene (56–59 Ma) age, which indicates this is the youngest of the terranes and is consistent with the interpretation of the tectonic setting. The mafic rocks from the Pouebo Terrane occur in a metamorphosed ophiolitic mélange, and have similar geochemical features to those of the Poya Terrane and to island arc tholeiites with a slightly enriched REE pattern and Nb depletion. The protoliths seem to be derived from the reworked Poya and island arc terranes. The Ophiolitique Nappe is underthrusted by the Poya and Pouebo Terranes and is mainly composed of harzburgite and dunite. This ultramafic allochthon is extremely depleted and cannot have been in equilibrium with a melt of MORB composition (Eissen et al., 1998). The Ophiolitique Nappe was the basement on which, not the Poya Terrane, but the arc (Loyalty Arc) was built (Cluzel et al., 2001).

The Tangihua Ophiolite Complex, informally known as the Northland Ophiolite, is situated in the north of North Island, New Zealand. It consists of basaltic pillow and massive lavas, sheeted dykes, plutonic gabbro, diorite and plagiogranite, cumulate layered ultramafic rocks and gabbros, harzburgites and lherzolites (Malpas et al.,

1992). The lavas are intercalated with siliceous mudstone and micritic limestone. Intercalated and interpillowed sedimentary rocks have macro- and micro-faunas with an age ranging from mid-Cretaceous to Paleocene (Brook et al., 1988). Basalts contain phenocrysts of plagioclase, clinopyroxene, orthopyroxene, and rare magnetites and titanites. Olivine-rich and hornblende-bearing basalts are rare (Nicholson et al., 2000). Most lavas have a slightly LREE-depleted REE pattern and negative Nb anomalies. Several lavas have a LREE-enriched REE pattern. The Tangihua Ophiolite was generated in an arc and a back-arc (Nicholson et al., 2000).

The thick oceanic crust (up to 15–20 km) of the Caribbean plate has bulk Ar-Ar ages of ca. 90 Ma and 75 Ma (Sinton et al., 1998). It has mostly REE patterns that range from slightly LREE-depleted through flat to slightly LREE-enriched; but a few are OIB-like and LREE-enriched (Kerr et al., 1997b; Sinton et al., 1998). Cretaceous lavas crop out on islands in the Caribbean Sea (Aruba, Curacao, Trinidad, Hispaniola, Jamaica and Cuba), in the Coastal borderlands of Venezuela, the Pacific coast of Costa Rica, the Azuero and Sona peninsulas and Caribbean coasts of Panama, and in the Central and Western Cordillera of western Colombia and Ecuador (Kerr et al., 1997b and references therein). They mostly have bulk Ar-Ar ages of ca. 90 Ma and 75 Ma that are coeval with the Caribbean plate (e.g., Sinton et al., 1998). Their REE and isotopic compositional diversity are similar to that of the Caribbean plate (e.g., Kerr et al., 1997a; Sinton et al., 1998; Thompson et al., 2003). The contemporaneity and geochemical similarity between the Caribbean Plate and the Cretaceous lavas that crop out within and around the Caribbean Sea and in Western and Central Cordillera suggest a genetic derivation. Moreover, on the island of Curacao and in the Central Cordillera (Kerr et al., 1996b, 1997a) picritic lavas belong to the Caribbean Plateau (e.g., Kerr and Tarney, 2005). The isotopic signature of the Caribbean Plateau basalts shows that they were generated in the Galapagos hotspot (Thompson et al., 2003). This is consistent with paleomagnetic data that indicate derivation from near-equatorial latitudes (Acton et al., 2000). Radiolarian species in chert beds exposed on the islands of the northern Caribbean margin indicate a Pacific rather than a Caribbean/Atlantic origin (Montgomery et al., 1994). The Caribbean Plateau was generated at the present-day Galapagos hotspot.

Lavas coeval with the Caribbean Plateau occur on Gorgona Island and at Serrania de Baudo on the Pacific coast of Colombia, and at Pinon and Pedernales-Esmeraldas in Ecuador (Kerr et al., 1997a; Sinton et al., 1998). Gorgona Island is well known for its unique occurrence of Phanerozoic komatiite. Although most coastal lavas are geochemically similar to those of the Caribbean Plateau, komatiites, picrites and basalts from Gorgona have more diverse REE patterns that range from strongly LREE-depleted to LREE-enriched (Kerr et al., 1996a, 1997a). Depleted lavas from Gorgona are isotopically distinguishable from those of the Caribbean Plateau (Thompson et al., 2003). The coastal lavas are tectonically separated from the Western Cordillera by island arcs (Kerr et al., 2002; Kerr and Tarney, 2005). Although the Gorgona and coastal lavas have been regarded as a part of the Caribbean Plateau, it has been suggested that these are part of another plateau termed the Gorgona Plateau (Kerr et al., 2002; Kerr and Tarney, 2005). The accretion ages are critical to settle the controversy.

On Gorgona Island middle Eocene marine sedimentary rocks occur in a fault-bounded block in contrast to Miocene and Oligocene unconformable deposits on lavas without tectonic disturbance (Kerr and Tarney, 2005); this suggests that the accretion age was Late Eocene. Tonalite batholiths from the island of Aruba in the Caribbean Sea have a biotite Ar-Ar age of 85–82 Ma (White et al., 1999), indicating Late Cretaceous accretion of the Caribbean Plateau (Kerr and Tarney, 2005). Paleomagnetic data for Gorgona Island indicate a provenance latitude of ~26°S (MacDonald et al., 1997). This is consistent with a longer duration of migration of the Gorgona Plateau compared with that of the Caribbean. Kerr and Tarney (2005) proposed that the Gorgona Plateau formed at the site of the present-day Sala y Gomez hotspot.

The East Sulawesi Ophiolite, Indonesia, has a crust with a minimum thickness of 8 km (Kadarusman et al., 2004). The most common basalts are aphyric; and minor porphyritic basalts have less olivine phenocrysts. Mineral chemistry of cumulate rocks clearly cannot indicate that the rocks are derived from an arc setting, although the geochemical features of the basalts indicate their suprasubduction origin. On the basis of the petrological and mineral chemical data, Kadarusman et al. (2004) suggested that the rocks were generated in an oceanic plateau. K-Ar dating of underlying mélange and metamorphic sole indicates it was generated at 138 Ma and emplaced before 28 Ma (Parkinson, 1998). The plateau can be tracked back to near the Pacific Superplume region at its formation age (Kadarusman et al., 2004).

The Iratsu and Higashi-Akaishi bodies that contain the highest grade rocks of the Sanbagawa metamorphic belt in southwestern Japan are composed of ultramafic rocks, eclogitic metabasites with a basalt-gabbro origin, metacarbonate, metachert and pelitic gneiss in ascending order (Maruyama et al., 2001; Terabayashi et al., 2005). The bodies are separated from their surrounding schists on the top by a roof thrust and on the bottom by a floor thrust. They have a duplex structure composed of four horses. The reconstructed OPS of the bodies suggests that they were derived from a huge oceanic plateau covered by pelagic limestone with minor chert on its flank (Maruyama et al., 2001; Kugimiya and Takasu, 2002). Metagabbros contain relics of high-pressure (i.e., garnet-bearing) granulite-facies and subsequent eclogite-facies metamorphism (Yokoyama, 1980). The petrological thickness of the plateau must have exceeded 30 km because of the occurrence of the relict high-pressure granulites in the lower horizons of the reconstructed stratigraphy. The Mikabu greenstone belt that extends for about 800 km along the southern margin of the Sanbagawa belt is mainly composed of mafic volcanic rocks and ultramafic-mafic cumulates (e.g., Ozawa et al., 1997). The Mikabu greenstones also underwent subduction-related high-P/T metamorphism, and are regarded as the low-grade part of the Sanbagawa belt (e.g., Banno and Sakai, 1989; Suzuki and Ishizuka, 1998). Their geology and petrochemistry including a HIMU signature (high-Nb/Zr and Nb/Y ratio; Ozawa et al., 1999) indicate that the Mikabu greenstones were derived from a seamount chain and/or oceanic plateau (Isozaki et al., 1990; Ozawa et al., 1999; Uesugi and Arai, 1999); i.e., they formed by superplume or plume activity. K-Ar dating of igneous amphiboles from the Mikabu gabbros (Ozawa et al., 1997), and U-Pb dating for zircons (inherited cores) from the Sanbagawa eclogites (Okamoto et al., 2004) combined

with microfossils from pelagic sediments associated with the greenstones indicate the Sanbagawa and Mikabu protoliths have eruption ages of 142–153 Ma (Sanbagawa: Isozaki and Itaya, 1990; Mikabu: Sakakibara et al., 1993). Metamorphic zircons from the Sanbagawa eclogites have U-Pb ages of 110–120 Ma; this points to the accretion age (Okamoto et al., 2004).

Greenstones from the Sorachi-Yezo belt in central Hokkaido, northern Japan have N-MORB- to E-MORB- and OIB-like geochemical features (Sakakibara et al., 1999; Nagahashi and Miyashita, 2002). Some OIB-like greenstones have high Nb/Y and Nb/Zr ratios (Sakakibara et al., 1999) and were generated from heterogeneous sources in an oceanic plateau (Kimura et al., 1994; Sakakibara et al., 1999). The radiolarian age of chert xenoliths in lavas is Latest Jurassic (ca. 150 Ma) and is regarded as close to the time of eruption (Sakakibara et al., 1999). Radiolaria from black shale in the top layer of the OPS including the Plateau indicate that the emplacement age was Barremian (Sakakibara et al., 1999). This oceanic plateau can be tracked back to the Pacific Superplume region (Kimura et al., 1994).

The Josephine Ophiolite in northern California and southern Oregon, US, contains pillow lavas overlain conformably by thin chert and thick turbidite and a sheeted dyke complex (Saleeby et al., 1982; Harper, 1984). Plagiogranite pods in gabbro-diorite and between sheeted dykes, and a dacite dyke that cuts both lavas and sediments have zircon U-Pb ages of 157 and 151 Ma, respectively (Saleeby et al., 1982). The former is regarded as the generation age and the latter the age of emplacement; the Josephine Ophiolite had a short time interval from generation to emplacement. Because the turbidites include andesitic clastics, the Josephine ophiolite is thought to have formed in proximity to an island arc (Saleeby et al., 1982; Harper, 1984). A marginal basin origin is indicated by earlier clinopyroxene crystallization based on the phenocryst assemblage of the lavas and the occurrence of orthopyroxene in cumulates (Harper, 1984). The trace element patterns of the lavas correspond to those from MORB to island arc tholeiite. The fact that the highest grade of hydrothermal metamorphism is amphibolite facies in cumulates indicates a relatively thin crust. We agree with Saleeby et al. (1982) and Harper (1984) that the above-mentioned data indicate that the Josephine Ophiolite was generated during the opening of a marginal basin. The Devils Elbow Ophiolite in western California has similar stratigraphic and geochemical features as the Josephine ophiolite and is regarded as its southern continuation; its zircon U-Pb age is 164 Ma (Wright and Wyld, 1986; Wyld and Wright, 1988). The marginal basin that generated the Josephine Ophiolite began to open by this time.

The Coast Range Ophiolite that crops out in scattered localities over a 700-km-long segment in western California contains two rock units. One is associated with minor felsic igneous rocks and shows island arc geochemical features and a zircon U-Pb age of 160–170 Ma (Shervais and Kimbrough, 1985). The other is a mélange with a serpentinite matrix and has MORB or seamount geochemical features and a Tuthonian radiolarian fauna in chert blocks (Shervais and Kimbrough, 1985). The first unit was generated in an island arc, and the second in a seamount. The Great Valley Group that overlies the Coast Range Ophiolite contains greenstones that have

similar geochemical features and radiolarian ages (MacPherson and Phipps, 1988), and seems to have an origin similar to the Coast Range Ophiolite.

Although many ophiolites and greenstones were generated in convergent regions, there are many ancient plateaus in accretionary prisms in circum-Pacific orogenic belts; the Caribbean Plateau, Gorgona Plateau, East Slawesi Ophiolite, Iratsu massif and Sorachi-Yezo belt. The eruption ages of these plateaus are dated as 75–150 Ma that is close to the peak age of the Cretaceous plateaus in the western Pacific. Considering their emplacement ages and durations of migration, the birth-place of these plateaus was directly or nearly on the Pacific Superplume region (Fig. 4). This indicates that the Pacific Superplume contribution to the Cretaceous pulse was much higher than previously estimated.

3.2 From 550 to 200 Ma

3.2.1 Continental domain

In this period, the history of continents was dominated by the amalgamation of the supercontinent Pangea (e.g., Ford and Golonka, 2003; Golonka et al., 2003; Windley, 1995, and references therein). The (semi-) supercontinent Gondwana and the three major cratons of Baltica (northeastern Europe), Laurentia (North America including Greenland, northern Scotland and northern Ireland) and Siberia were dispersed in Cambrian (Fig. 5). Laurentia collided with Baltica in the Silurian (East Greenland Caledonian and Scandian orogenies). The suture of Laurentia with Avalonia that had departed from the northern margin of Gondwana also formed at this time (Acadian

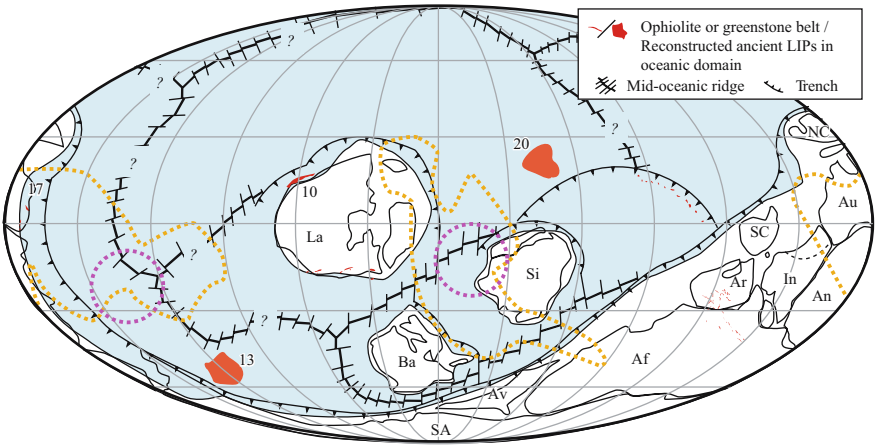


Figure 5. Reconstructed paleogeographic maps at ca. 500 Ma. The distribution of continents is refered to Scotese (2004). Numbers of ophiolites or greenstone belts are shown as Figure 2. Af = Africa; Ar = Arabia; An = Antarctica; Au = Australia; Av = Avalonia; Ba = Baltica; In = India; La = Laurentia; NC = North China; SA = South America; SC = South China; Si = Siberia.

orogen). A series of collisions between Laurentia, Baltica and Avalonia resulted in closure of the Iapetus Ocean and formation of Laurussia. Prior to these collisions, Pacific-type orogens developed in the Cambrian (e.g., Penobscotian and Finnmarkian orogenies). Laurussia collided with the western and central European blocks from the Devonian (Hercynian/Variscan orogen). Meanwhile, the most extensive juvenile additions to the crust in the Phanerozoic took place around the western, eastern and southern margins (present-day coordinates) of Siberia, and involved continental fragments separated from the northern margin of Gondwana (the Central Asian Orogenic Belt, Jahn et al., 2000, 2004). The Kazakhstan block that mainly consists of Neoproterozoic and early Phanerozoic juvenile crusts (Heinhorst et al., 2000) converged with Siberia in the Early Carboniferous. The collision of Kazakhstan/Siberia with Laurussia occurred in the Late Carboniferous (Uralian orogen) and resulted in the formation of Laurasia that became a northern part of Pangea. The final formation of Pangea was caused by the collision of Laurasia and Gondwana in Late Carboniferous-Early Permian time (Alleghenian and West African orogens).

The Pacific Ocean has been closing along its eastern (Cordilleran, western North America) and western margins (Tasmanide, Western Australia) since the Cambrian (Fig. 5). The Paleo- and Neo-Tethyan Oceans developed as Indian-type oceans that have one-side subduction (Figs. 6 and 7). These oceans transported the continental fragments separated from the Gondwana margin to Laurentia, Baltica and Siberia. Laurentia was subducted along both its eastern and western sides and a V-shaped subduction zone, like that in the present-day Western Pacific, was formed around

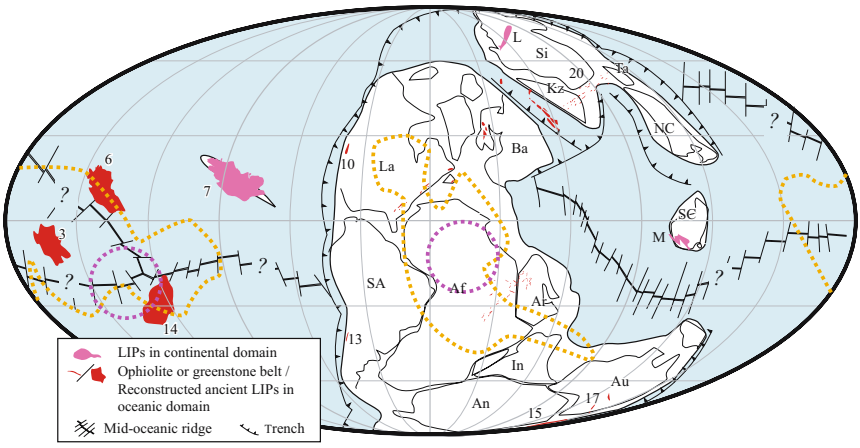


Figure 6. Reconstructed paleogeographic maps at ca. 250 Ma. The distribution of continents is mainly refered to Scotese (2004) but we divided Kazakhstan from Baltica because final event of Uralian orogeny occurred during the Triassic and Early Jurassic (Golonka et al., 2003). Alphabets of LIPs and numbers of ophiolites or greenstone belts are shown as Figure 2. Af = Africa; Ar = Arabia; An = Antarctica; Au = Australia; Ba = Baltica; In = India; Kz = Kazakhstan; La = Laurentia; NC = North China; SA = South America; SC = South China; Si = Siberia; Ta = Tarim.

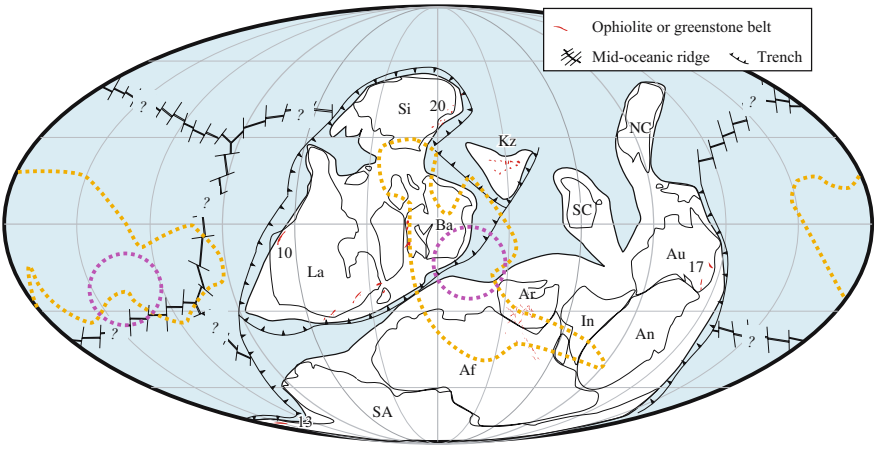


Figure 7. Reconstructed paleogeographic maps at ca. 400 Ma. The distribution of continents is mainly refered to Scotese (2004) but we divided Laurentia from Africa because Alleghenian and Western African orogen was developed during Late Carboneferous and Earky Permian (Ford and Golonka, 2003). Numbers of ophiolites or greenstone belts are shown as Figure 2. Af = Africa; Ar = Arabia; An = Antarctica; Au = Australia; Ba = Baltica; In = India; Kz = Kazakhstan; La = Laurentia; NC = North China; SA = South America; SC = South China; Si = Siberia.

this craton. This Paleozoic plate conversion and the resultant formation of Laurussia occurred in the African Superplume region (Fig. 7).

Continental flood basalts erupted in two regions at the Permian-Triassic boundary; the Siberian Traps at 251.2 ± 0.3 Ma (Kamo et al., 1996), and the Emeishan flood basalts in South China at 251–253 Ma (Lo et al., 2002). These differ from the Mesozoic continental flood basalts; they were generated far from superplume regions (Fig. 6), and failed to develop to continental breakup (Courtillot et al., 1999).

3.2.2 Oceanic domain

A large Triassic greenstone belt in the Wrangellia Terrane extends from Vancouver Island in British Columbia to southern Alaska. It consists of subaerial flows, pillow basalts, but no sheeted dykes and is overlain by cherts and middle Ladinian limestones and by late Karnian and early Norian limestones (Jones et al., 1977). The thickness of this Triassic greenstone is up to ~7000 m (Lassiter et al., 1995). It overlies Pennsylvanian to early Permian volcanics and sedimentary rocks belonging to an island arc (Jones et al., 1977). The greenstones have an E-MORB-like geochemical signature (Davis and Plafker, 1984) but suffer isotopically from crustal contamination (Lassiter et al., 1995). These geologic and geochemical features indicate that the Triassic greenstones in the Wrangellia Terrane were flood basalts on top of an island arc.

In a low-grade metamorphic complex in the Andes of Aysén, southern Chile pillow basalts from the Chonos metamorphic complex contain turbiditic pelitc-psammitic schist intercalations (Hervré et al., 1999). The deposition age of the turbidites is Late

Triassic. The basalts have a phenocryst assemblage of clinopyroxene and plagioclase and E-MORB-like geochemical features (Hervé et al., 1999). Although geochemical, geologic and geochronological evidence is minor, this complex may have been derived from an oceanic plateau setting. Paleozoic pillow basalts from the Eastern Andes metamorphic complex occur as blocks together with marbles in turbiditic sediments (Hervé et al., 1999). They are correlated with the Late Devonian Bahia de la Lancha formation in Argentina. The basalts have small phenocrysts of clinopyroxene and plagioclase, enriched REE patterns and high Nb/Y ratios. Their Nb/Y ratios are comparable with those in Polynesian basalts. We consider the basalts are OIB related to a superplume.

The Yakuno Ophiolite in Southwest Japan contains plagiogranite with a zircon U-Pb age of 282–285 Ma (Herzig et al., 1997). Associated amphibolites have Permian K-Ar and Rb-Sr ages that date the time of low-pressure metamorphism prior to emplacement (Ishiwatari, 1985b). Basaltic pillow lavas are intercalated with black shales and felsic volcanics; sheeted dykes are absent (Ishiwatari, 1985a,b). The basalts are mostly aphyric, although olivine and plagioclase phenocrysts (both are pseudmorphed) are present. The chemistry of whole rocks, relict clinopyroxene, and relict chromian spinel all indicates a tholeiitic affinity. Downward increase of the metamorphic grade up to the pyroxene-granulite facies indicates that the oceanic crust was unusually thick. Although Ishiwatari (1985a) suggested the ophiolite was derived from a small oceanic basin like the Black Sea, it is more likely that it was an oceanic plateau in origin (Isozaki, 1997).

Greenstones from the Angayucham Terrane, central Alaska are overlain by thin chert beds (Pallister et al., 1989). The radiolaria from inter-pillowed chert points to a Mississippian deposition age (Barker et al., 1988). The greenstones are E-MORB-like tholeiites (Barker et al., 1988; Pallister et al., 1989). According to the geologic and geochemical data, these rocks are an oceanic plateau in origin. Subsequently, the plateau became occur according to radiolarian ages and finally arrived at the Brooks Range in Alaska in the Middle Jurassic (Pallister et al., 1989).

The Dun Mountain Ophiolite has a length of >1100 km in the South Island, New Zealand. The igneous rocks are divided into three: 1) a lower sequence of olivine-phyric pillow lavas and autobrecciated flows and comagmatic intrusives, 2) an upper sequence of massive and brecciated, predominantly aphyric, augite and Fe-Ti oxide-bearing basaltic sheeted flows, 3) a suite of cross-cutting (non-sheeted) mafic dykes and small irregular plutons, layered ultramafics and gabbroic cumulates, isotropic gabbros, and abundant plagiogranites dykes and plutons (Sivell and McCulloch, 2000). Plagiogranite has a zircon U-Pb age of 275–285 Ma (Kimbrough et al., 1992). Mafic dykes and plagiogranites from the suite have a Sm-Nd bulk isochron age of 278 ± 4 Ma (Sivell and McCulloch, 2000), while the upper sequence has a Sm-Nd bulk isochron age of 308 ± 12 Ma on basalt and related ferrogabbro. The Dun Mountain Ophiolite lacks thick pelagic chert but has voluminous terrigenous sediments, although the upper sequence is conformably overlain by red cherts, Fe-Mn-rich nodular encrustations, red mudstones and altered hyaloclastites, and thick turbidite argillites (Sivell, 2002). Lavas from the lower sequence are typically olivine-phyric

and have LREE-enriched REE patterns, high Nb contents and enriched Nd isotopic compositions. Massive lava flows from the upper sequence have LREE-depleted REE patterns, negative Nb anomalies and slightly depleted Nd isotopic compositions. A suite of dykes and plutons have a LREE-depleted REE pattern, a negative Nb anomaly and a depleted Nd isotopic composition (Malpas et al., 1994; Sano et al., 1997; Sivell and McCulloch, 2000). The lower and upper sequences and the suite of dykes and plutons are similar in geochemistry to OIB, back-arc basin basalt, and island arc tholeiite, respectively. Although Malpas et al. (1994) considered that lavas from the lower sequence formed in a seamount in a mid-ocean, Sivell and McCulloch (2000) concluded that together with the basalts they were akin to back-arc basin basalts and favored generation in a seamount in a back-arc basin. Dykes and plutons represent incipient arc magma intruding preexisting back-arc-basin crust at an initial subduction (Sivell and McCulloch, 2000).

Cambrian ophiolites occur throughout the Tasmanides of eastern Australia. Ophiolites in the Tyennan and Delamerian orogens near the western margin of the Tasmanides have a zircon U-Pb age of 514 Ma on tonalite and 524 Ma on leucogabbro (Black et al., 1997; Maher et al., 1997). Lavas in the Tyennan orogen are pillowed or massive low-Ti basalts and boninites and cumulates are orthopyroxene-rich (Crawford and Berry, 1992). The basalts have a LREE-depleted REE pattern and low Ti, Nb, and Zr contents. Mafic-ultramafic complexes of the Dimboola subzone in the Delamerian orogen have petrological and geochemical characteristics similar to those of the Tyennan orogen (Maher et al., 1997). The Lachlan orogen that occupies the central Tasmanides has two major ophiolitic belts; Heathcote and Mount Wellingston. The Heathcote belt contains a conformable sequence of basalt, chert-shale-volcanoclastic sandstone, and quartz-rich turbidite, within which tuffeceous litherenite has a zircon U-Pb age of 503 Ma (Spaggiari et al., 2003). Volcanic rocks consist of basalts, boninites and andesites; the basalts have flat REE patterns and geochemical characteristics between MORB and arc tholeiite (Crawford and Keays, 1987). The Mount Wellingston belt has a zircon U-Pb age of 502 Ma from hornblende gabbro (Spaggiari et al., 2003). Volcanic rocks are basalts and boninites. The pillow basalts are conformably overlain by and interbedded with chert and silicified black shale, which in turn is conformably overlain by turbidite. Basalts have flat REE patterns and geochemical characteristics between MORB and arc tholeiite and are similar to those in the Heathcote Belts (Crawford and Keays, 1987). The New England orogen that is situated in the eastern Tasmanides has Neoproterozoic and Cambrian ophiolites. The Marlborough block consists of dominant serpentinized harzburgite and minor dunite, pyroxenite, gabbro, and mafic and felsic intrusive rocks (Bruce et al., 2000). Basalts have depleted MORB-like geochemical and isotopic signatures and a whole-rock Sm-Nd isochron age of 562 Ma. Ophiolitic mélange from the Peel-Manning Fault system contains basalts that have geochemical affinities with MORB to island-arc basalt, and lower-Ti and high-Mg island-arc- or fore-arc-basalt signatures (Yang and Seccombe, 1997). Plagiogranite blocks in a serpentinite matrix have zircon U-Pb ages of 530, 509, and 535 Ma (Aitchison et al., 1992; Aitchison and Ireland, 1995). These are suprasubduction zone ophiolites that developed along the

East Gondwana active margin from the Latest Neoproterozoic to the Late Cambrian (Crawford and Berry, 1992; Spaggiari et al., 2003).

The Wrangellia Terrane comprises a flood basalt erupted on an island-arc basement. According to paleomagnetic data, the terrane was positioned somewhere in the eastern Pacific Ocean and detached from the eastern margin of Laurentia at a paleolatitude of 10°N–20°N in the Late Triassic (Butler et al., 1997). The flood basalts were erupted near the Pacific Superplume region. The Permian Angayucham Terrane and Yakuno Ophiolite were regarded as the remnants of an oceanic plateau. Although there is little supporting evidence, the basalts from Chonos metamorphic belt might also have formed in an oceanic plateau. These generation ages are nearly coeval with those of the Wrangellia Terrane (230–290 Ma). Although there are no available paleomagnetic data for these greenstones and ophiolite, by comparing their data with those from the Cretaceous oceanic plateaus in western Pacific, it could be concluded that they were generated in the region of the Pacific Superplume (Fig. 6).

3.3 From 750 to 550 Ma

3.3.1 Continental domain

In the period from 550 to 750 Ma the supercontinent Rodinia brokeup and this led to the formation of the (semi-) supercontinent Gondwana (Hoffman, 1991; Dalziel, 1992). The formation of Gondwana was likely caused by a rapid fan-like closure of the Mozambique Ocean that was present between Eastern and Western Gondwana, and it was dramatically completed by the collisional 550–500 Ma Mozambique orogeny that represents the final event of the Pan-African orogen (Dalziel, 1992; the "Inside-out model" by Hoffman, 1991). However, recent geochronological data require us to revise our ideas about the distribution of the Pan-African orogen and the formation model of Gondwana. One of the important points of the previous model was that Eastern Gondwana was a stable large continent in the period concerned in East Antarctica that constitutes the core of Eastern Gondwana. Pan-African orogens have recently been subdivided into three provinces (Shiraishi et al., 1994; Fitzsimons, 2000). According to their ages, Eastern Gondwana was not present until 530 Ma (Meert, 2003). The qualitative and quantitative geologic and geochronological data from the Pan-African orogens in the African and South American continents revealed that the formation of Western Gondwana was not completed until 520 Ma (e.g., Campos Neto, 2000). This refers to the idea that Gondwana was formed by the collision of several cratons in sequence rather than by a simple collision between two large continents. This mode of continental amalgamation is comparable with that of Laurasia in the Phanerozoic.

Did Gondwana include Laurentia or was there are a Latest Proterozoic supercontinent termed Pannotia (Dalziel, 1997)? This question is related to the time of the opening of the Iapetus Ocean. The remnants of the opening stages of the Iapetus Ocean in the Laurentia, Baltica, and Amazonia cratons that surround the ocean are dated as ca. 600 Ma (Hoffman, 1989; Svenningsen, 2001). This age indicates that the

birth of the Iapetus Ocean was followed by the completion of Gondwana formation. The Baltica and Siberia cratons also departed from Gondwana. Therefore, we regard Gondwana not as a supercontinent but as a semi-supercontinent.

The breakup of Rodinia and the opening of the Pacific Ocean occurred at ca. 750 Ma (Fig. 8). The initial stage is represented by dyke swarms and associated volcanism; the Gairdner dyke swarm in central Australia at 827 ± 6 Ma (Wingate et al., 1998), the Amata dyke swarm in south-central Australia at 824 ± 4 Ma (Sun and Sheraton, 1996), the Mundine Well dyke swarm in northwestern Australia at 755 ± 3 Ma (Wingate and Giddings, 2000), the Sanfang mafic intrusive in South China at 828 ± 7 Ma (Li et al., 1999), the Richtersveld Igneous Complex in eastern South Africa at 833 ± 2 Ma (Frimmel et al., 2001), the Gunbarrel mafic magmatic event in eastern Laurentia at 780 ± 1 Ma (Harlan et al., 2003), and the Franklin dyke swarm at $723 + 4/-2$ Ma in northern Laurentia (Heaman et al., 1992). According to the reconstruction of continental distributions by the PALEOMAP project (Scotese, 2004), these events occurred in today's Pacific Superplume region (Fig. 8). In the period from 750 to 650 Ma, Rodinia was almost surrounded by Pacific-type orogenic belts. The Cadomian, Avalonian, Timanian, and Baikalian orogens developed along the margin of Western Africa, Amazonia, Baltica, and Siberia, respectively (e.g., Egal et al., 1996; Doig et al., 1993; Kuzmichev et al., 2001; Scarrow et al., 2001;

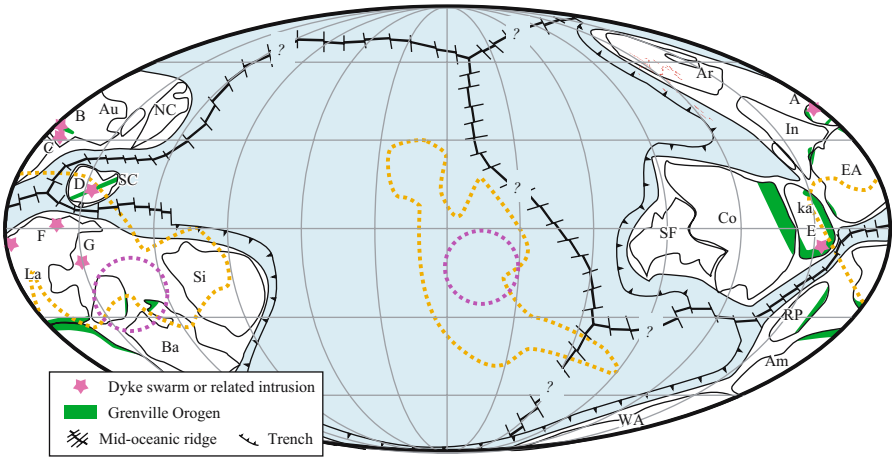


Figure 8. Reconstructed paleogeographic maps at ca. 750 Ma. The distribution of continents is mainly refered to Scotese (2004) but the South China was positioned on the basis of the reconstruction of Li and Powell (2001). According to the age of the Richtersveld Igneous Complex (Frimmel et al., 2001), Kalahari was separated from the Rodinia. The distribution of Grenville orogen is modified after Hoffman (1991). A = Mundine Well dyke swarm; B = Amata dyke swarm; C = Gairdner dyke swarm; D = Sanfang mafic intrusive; E = Richtersveld Igneous Complex; F = Gunbarrel mafic magmatic event; G = Franklin dyke swarm. Am = Amazonia; Ar = Arabia; Au = Australia; Ba = Baltica; Co = Congo; EA = East Antarctica; In = India; Ka = Kalahari; La = Laurentia; NC = North China; RP = Rio de la Plata; SC = South China; SF= Sao Francisco; Si = Siberia; WA = West Africa.

Khain et al., 2003). The early stage of the Pan-African orogen developed around the Sao Francisco-Congo craton (e.g., Campos Netro, 2000; Pimentel et al., 1991), and the extensive juvenile crust of the Nubian-Arabian shield was formed (Stein and Goldstein, 1996).

3.3.2 Oceanic domain

The Trinity Ophiolite that formed from the Cambrian to the Silurian is situated in eastern Klamath, northern California in western North America. In the Lovers Leap-South China Mountain area plagiogranite has a zircon U-Pb age of 565–570 Ma (Wallin et al., 1988). Lavas consist of basalt, andesite, and dacite, all of which have plagioclase and clinopyroxene phenocrysts, and orthopyroxene is present in a few andesites (Brouxel et al., 1989). Hornblende phenocrysts occur in dacitic andesites and dacites. The lavas are divided into two types based on their geochemical features. One is low-K tholeiite with a depleted REE pattern and the other is calc-alkaline with an enriched REE pattern. The calc-alkaline rocks are conformably overlain by Ordovician limestones. Both low-K tholeiite and calc-alkaline rocks have negative Nb anomalies (Brouxel et al., 1989). Well-developed sheeted dykes are absent (Lindsley-Griffin, 1994). Pegmatitic trondhjemite dykes that intrude gabbro have a zircon U-Pb age of 412 Ma (Wallin et al., 1988). In the Dunsmuir area a complete ophiolitic succession is present. Nd isotopic ratios measured on basalt, plagiogranite, isotropic gabbro, cumulate layered gabbro, and gabbroic pegmatite plot on 452 ± 40 Ma isochron (Brouxel and Lapierre, 1988). The peridotite layer has unusually large amounts of lherzolite (Brouxel and Lapierre, 1988) and some lherzolites and harzburgites have high plagioclase contents (Lindsley-Griffin, 1994). A sheeted dyke complex (Brouxel and Lapierre, 1988) occurs with predominant basaltic pillow lavas that are unconformably overlain by Carboniferous sandstone and shale. The basalts are divided into three types based on their petrography; plagioclase-porphyritic basalts with rare clinopyroxenes, intersertal basalts with clinopyroxene microphenocrysts and plagioclase laths, and subaphyric basalts with clinopyroxene microlites (Brouxel et al., 1989). The lavas of these basalts have depleted REE patterns and negative Nb anomalies (Brouxel et al., 1989). In the Redding area massive and pillowed flows are overlain by rhyolites, and are unconformably overlain by Early Devonian shales and limestones (Brouxel et al., 1988). The flows consist of basalts and andesites that are highly porphyritic with plagioclase, olivine and clinopyroxene phenocrysts (Brouxel et al., 1989). The basalts and andesites show a significant geochemical heterogeneity that is indicated by variable REE patterns that range from moderately depleted to strongly enriched (Brouxel et al., 1988), and they have negative Nb anomalies (Brouxel et al., 1989). High-Mg andesites have $SiO_2 \geq 55\%$, $MgO \geq 7\%$, and flat REE patterns (Brouxel et al., 1988). The above geochemical characteristics suggest that the Trinity Ophiolite was generated in an island arc-marginal basin (Brouxel and Lapierre, 1988; Brouxel et al., 1988, 1989).

A highly deformed mafic-ultramafic complex is situated in the southwestern margin of the Precordillera of Argentina. It is divided into three tectonic units; a gabbro, microgabbro, and diabase unit (massive diabase), an ultramafic and layered gabbro

complex that intrudes quartzofelspathic gneiss (ultramafic-layered complex), and metasedimentary rocks with interlayered mafic flows and sills. Based on geochemistry, metamorphism and geochronology, these units are unrelated to each other and cannot represent a fragmented single ophiolite (Davis et al., 2000). The massive diabase unit consists of gabbro to diabase bodies with small plagiogranite and sheeted half dykes with pillow lavas. Sedimentary rocks are not associated with pillow lavas (Gregori and Bjerg, 1997; Davis et al., 2000). This unit has a zircon U-Pb age of 576 ± 17 Ma from microgabbro (Davis et al., 2000). The lavas and dykes have REE patterns that range from flat through slightly LREE-enriched to enriched patterns and no negative Nb anomaly (Gregori and Bjerg, 1997). These were interpreted to form at a mid-oceanic ridge associated with a plume (Gregori and Bjerg, 1997) or at a well-developed rift (Davis et al., 2000). But the geochemical signature of the massive diabase unit is also similar to that of an oceanic plateau. Present-day western margin of South America was faced to the Pacific Ocean in this period. Therefore, it is possible that the massive diabase unit in the southwestern margin of the Precordillera was generated at the Pacific Superplume region.

A Cambrian accretionary complex in the Gorny Altai Mountains in southern Siberia continues in the Altai Range through Mongolia to China. The accretionary complex is composed of limestone, greenstone, sandstone and mudstone (Buslov et al., 1993; Buslov and Watanabe, 1996). The Baratal limestone in the Kurai area has a $^{207}Pb/^{206}Pb$ bulk isochron age of 598 ± 25 Ma, and has a primary stratigraphy made-up of massive limestone and limestone breccia that conformably overlies basaltic greenstones (Uchio et al., 2004). Some limestones contain stromatolites and ooids that suggest a shallow-marine environment. Some limestone breccias contain clasts of micritic limestone, greenstone and chert, and are poorly sorted and thinly bedded, suggesting that they formed as gravity-flow (debris flow) deposits. In addition, laminated limestone and bedded micritic limestone are associated with the limestone breccias. The absence of coarse-grained terrigenous clastics indicates that all the limestones were deposited in a mid-oceanic environment distant from a continental source. The Baratal limestone is interpreted as a paleoseamount limestone that accumulated on MORB- and OIB-type basaltic greenstones (Buslov et al., 1993). Most of the greenstones have phenocrysts of clinopyroxene and plagioclase. The above evidence suggests that the limestones accumulated on the slope or at the base of a slope of a paleo-seamount or plateau (Dobretsov et al., 2004; Uchio et al., 2004).

A Precordilleran ophiolite in Argentina might be a fragment of an ancient oceanic plateau. The greenstones in the Gorny Altai area of southern Russia have an oceanic plateau affinity. Although the Central Asian Orogenic Belt that includes the Gorny-Altai region faced the Tethyan Ocean, the accretionary prism developed along an oceanic island arc and could have faced the Pacific Ocean (Fig. 5). The oceanic plateau might have formed in the Pacific Superplume region. Their ages are nearly coincident (ca. 580–600 Ma). While there are no available paleomagnetic data for these ophiolite greenstone belt, by comparing them with the Cretaceous pulse, we can conclude they were generated in the Pacific Superplume region.

4 DISCUSSION

4.1 The reconstruction of rodinia and initial opening of the pacific ocean

Our reconstructions and discussion are tentatively based on the PALEOMAP project maps (Scotese, 2004) but the continental arrangement of Rodinia has not yet reached a consensus; thus it is necessary to consider other reconstructions. Although many papers concerned with Rodinia have been published since the proposal by Hoffman (1991) and Dalziel (1991), due to space limitations we keep this review to a minimum so as to extract the essence of the consensus and arguments.

Because of the presence of Grenvillian-age orogens within the cratons, the connections between Baltica, Amazonia, and Rio de La Plata with Laurentia are broadly accepted. It is also widely accepted that Siberia was connected to northern Laurentia, but there has been little agreement on the geometry of the fit due to a lack of decisive paleomagnetic or geochronological data. Kravchinsky et al. (2001) pointed out that the Siberian platform, composed of the Anabar, Angara and Aldan blocks, might not have been fully amalgamated by Late Proterozoic to Early Cambrian time.

To explain the paleoposition of East Gondwana (Antarctica, Australia and India) against Laurentia in Rodinia, three models have been proposed: (1) East Antarctica (Transantarctic Mountains) was connected with the southwestern coast of Laurentia. This is based on correlations of Grenville-age orogens and Precambrian-Paleozoic sedimentary rocks (the SWEAT model: Moores, 1991; Dalziel, 1991; Hoffman, 1991; Young, 1992), and the idea that South China was placed among Australia and Laurentia-Siberia (Li and Powell, 2001). Powell et al. (1993) argued against the validity of the SWEAT model with APWPs for both East Gondwana (mainly from Australia and partly from India) and Laurentia, and Li (2000) and Wingate and Giddings (2000) supported this idea from the viewpoint of the APWPs for western Australia and Laurentia. (2) A suture along the eastern coast of India, the eastern coast of East Antarctica and the central-southwestern part of Australia continued into the Grenville orogen through the southern end of Laurentia, and Australia was connected with western Laurentia (the AUSWUS model: Karlstrom et al., 1999, 2001; Burrett and Berry, 2000). In this model South China was separated by small oceans from Australia and Siberia (Condie, 2003). Karlstrom et al. (2001) suggested that the AUSWUS model provided a better fit of paleomagnetic data (APWP) than the SWEAT model. (3) A model with the Australia-Mexico connection (AUSMEX), inferred from ca. 1070-Ma paleopoles from Australia with a high-stability paleomagnetic remanence (Wingate et al., 2002). On the other hand, from zircon U-Pb data and geologic correlations Fitzsimons (2000) and Boger et al. (2001) suggested that East Antarctica should be separated into two or three provinces with a Grenville-age by Pan-African orogens. In addition, Powell and Pisarevsky (2002) pointed out that India lay near the pole, whereas Australia was at a low latitude at 810 Ma, and final amalgamation of East Gondwana was not complete until the Early Cambrian. Considering these suggestions, Pisarevsky et al. (2003) proposed a new reconstruction of Rodinia at 990 Ma, in which the AUSMEX model was adopted, and India was

excluded from Rodinia. However, the AUSWUS and AUSMEX models suggest that up to 10,000-km of Late Proterozoic rift margins in northern Australia and western Laurentia need to be matched with other continental blocks within any proposed Rodinia. As for the paleoposition of India, Radhakrishna and Joseph (1996) placed India near the equator at ca. 1000 Ma, suggesting a Late Proterozoic East Gondwana as before. On the other hand, Pisarevsky et al. (2003) disproved of this reconstruction due to the inconsistency between paleopoles of India and Australia at ca. 1070 Ma, although the APWPs of India from 1100 to 800 Ma were not available.

The recent accumulation of more precise paleomagnetic and geochronological data has provided several constraints and new models for Late Proterozoic reconstructions; however the controversy about East Gondwana and Rodinia has become more complicated. Each model has both advantages and disadvantages. At present, although it is still difficult to evaluate the validity of the recent reconstruction models, it can be emphasized that Laurentia was positioned in the center of Rodinia in all versions.

Figure 9 shows various models for the opening of the Pacific Ocean. The timing and distribution of rift systems depends not only on the age and dispersal of dyke swarm, but also on the arrangement of continents. Maruyama (1994) first proposed that the Pacific Superplume generated the Paleo-Pacific Ocean at 600–700 Ma on the basis that the paleolatitude of the RRR triple junction that was at ca. 20°S, corresponding to the active region of the present Pacific Superplume, and to the paleoposition of the Pacific superplume at the RRR triple junctions between western Laurentia, Australia and South China, and between the northern Laurentia, South China and Siberia (Fig. 9a). Li et al. (1999) and Li and Powell (2001) showed a similar triple

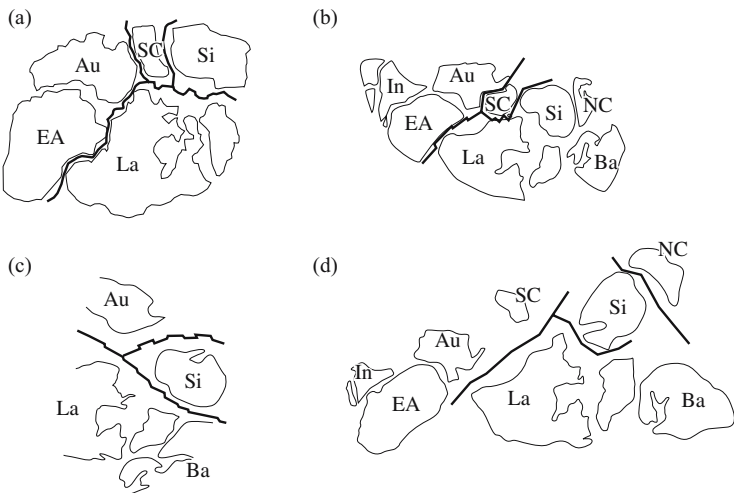


Figure 9. Paleogeographic reconstruction models of the supercontinent Rodinia. (a) After Maruyama (1994); (b) Li and Powell (2001); (c) Dobretsov et al. (2002); (d) after Condie (2003). Bold lines show rifts. Abbreviations of name of cratons are explained as in Figure 8.

junction at ca. 760 Ma, and suggested a mantle plume beneath South China (Fig. 9b). Dobretsov et al. (2003) provided stepwise rifting from 950–800 Ma between Australia and Siberia through 750–700 Ma rifting between Siberia and Laurentia and finally to an RRR triple junction between the three cratons (Fig. 9c). Condie (2003) produced a different model based on the AUSWUS model from other reconstructions based on the SWEAT model (Fig. 9d). But this also has a RRR triple junction at the opening of the Pacific Ocean. The RRR triple junctions are recognized in all reconstructions although the defining cratons differ from one to another. Using the analogy of the African rift system, an RRR triple junction is the expression of continental rift caused by plume upwelling (see summary by White and McKenzie, 1989). The paleolatitudes of RRR triple junctions vary from 30°N to 20°S. Because the uncertainty of paleolatitude estimation is up to 30° in this period (Scotese, 2004), the positions are roughly in agreement in the equatorial area. Although, in principle, paleolongtitude is not defined only by paleomagnetism, the reconstructed Rodinia of the PALEOMAP project at 750 Ma is in the Pacific Superplume region. According to the paleopole data of Weil et al. (1998, 2004), Laurentia occupying the central part of Rodinia moved to the south by ∼20° at ca. 800 Ma from the position at 750 Ma. This means that the initial rifting of Rodinia occurred in the Pacific Superplume region.

4.2 Comparison of the Pacific superplume with the African superplume

Associated with extensive flood basalt volcanism, the dispersal of Pangea occurred at 80–200 Ma on the African seismic lower velocity zone in the lower mantle that exists today. The relation of continental breakup with plume initiation has been mentioned by previous workers on the basis of analogue experiments of mantle convection and hot spot tracks (e.g., Morgan, 1981; Richards et al., 1989). Richards et al. (1989) suggested that a number of new mantle plumes were formed in this period. These are essentially independent and have no relation with one another. Each plume head generated flood basalts, subsequently plume tail activities left hot spot tracks. The model needs a number of narrow conduits from the core-mantle boundary, but it is not consistent with recent mantle tomographic images with higer resolution (e.g., Zhao, 2004). The seismic observations make us infer that the continental fragmentation was caused by cognate plume upwellings rooted in the upwelling lower mantle. This view is similar to the hotspot image provided by Courtillot et al. (2003). In analogy with Pangea, the fragmentation of Rodinia at 720–830 Ma arose in the Pacific. The breakup of a supercontinent is caused by superplume activity.

Dalziel et al. (2000) insisted that Pangea was fragmented by a preexisting plume. But the present position of the African superplume overlaps in paleo-latitude with the region where the 300–500 Ma orogens have been present. Pangea was formed by extensive collision-amalgamation processes around Laurentia after Pacific-type orogens were developed in the region. The eastern and western Laurentian margins underwent subduction both from the Pacific and Iapetus Oceans with the resultant formation of V-shaped Pacific-type orogens. This means that mantle downwelling rather than plume upwelling was provided by cold subducted slabs and is not consistent

with the model of Dalziel et al. (2000). During the formation of Rodinia, a large amount of oceanic lithosphere would have been subducted beneath proto-Rodinia along V-shaped paleo-trenches of the proto-Grenville orogens that were positioned on the Pacific Superplume region. These correlations suggest that the birth of a superplume was related to the formation processes of supercontinents, which include the Pacific-type orogeny along V-shaped subduction zones and the resultant collage of island arcs. The concentration of oceanic plate subduction during the formation process of a supercontinent could have greatly accelerated to create physical instabilities and chemical heterogeneities in the deep mantle, either or both of which must be deeply concerned with the birth of a superplume. There is no viable model with a consensus, however the transportation of oceanic lithosphere into the deep mantle most likely played an essential role in the birth of a superplume.

4.3 Superplume pulse

Cretaceous oceanic plateaus are widespread in the present western Pacific (e.g., Ontong Java Plateau, Manihiki Plateau, Hess Rise), and most formed at 75–150 Ma. In addition, the accreted fragments of oceanic plateaus in circum-Pacific orogens are coeval (Table 3). They can be traced back and found to be concentrated in the present active region of the Pacific Superplume (Fig. 4; Suzuki et al., 2000). This suggests that a large amount of igneous rocks (10.7×10^6 km^2 and 19.1×10^7 km^3) was formed in the Cretaceous by superplume activity. It is larger than the Australian continent (7.6×10^6 km^2).

In the mid-Cretaceous, most global changes of the surface environment can be comprehensively explained by the activities of the Pacific Superplume (Larson, 1991a,b); the Cretaceous global transgression was caused by a rise of sea level due to increasing spreading rates of mid-oceanic ridges, and the resultant young oceanic lithosphere was related to the Pacific Superplume activity. Cretaceous global warming also resulted from increasing rates of degassing by an extensive volcanism related to the superplume activity. In our estimation, the total amount of CO_2 derived from magmatism at that time is 2.8×10^{21} g, where the CO_2 contents in plateau basalt was assumed to be 0.5 wt% (Johnson et al., 1994). Kerrick and Caldeira (1993) concluded that over a 1-million-year period, excess CO_2 degassing of $>0.5 \times 10^{18}$ mol would be required to produce notable grobal warming. The degassing rate of CO_2 deduced from our composite volcano (0.82 10^{18} mol/m.y.) suggests a significant impact for Cretaceous global warming. In addition, excess CO_2 could be expelled by increasing spreading rate of mid-oceanic ridge (Larson, 1991a) and the coinciding formation of vast granite batholith in circum-Pacific belts (e.g., Wu et al., 2005).

From our review of circum-Pacific ophiolites and greenstone belts we infer that events such as the Cretaceous pulse occurred at 230–280 and 580–600 Ma, after the birth of the Pacific Ocean. Recent knowledge from ultrahigh-pressure experiments enables us to speculate with the following model for the active volcanism in the Pacific (Fig. 10). Phase relations in a mantle peridotite system (Zhang and Herzberg, 1994;

Table 3. Summary of the Cretaceous LIPs and their accreted fragments in the Pacific Ocean

Name	Age (Ma)	Area (10^5 km^2)	Volume (10^6 km^3)	Reference (age)	Reference (volume)
Ontong java plateau	90, 122	16	53	Mahoney et al., 1993	Richardson et al., 2000
Nauru basin	110.8	18	0.9	Castillo et al., 1994	Eldholm and coffin, 2000
East mariana basin	114.6	5	0.25	Pringle, 1992	Coffin, Eldholm, 1994
Pigafetta basin	126.1				
Manihiki plateau	91–114	8	8.8	Lanphere and Dalymple, 1976	Eldholm and coffin, 2000
Magellan rise	~135	5	1.8	Winterer et al., 1973	Eldholm and coffin, 2000
Hess rise	99–112	8	9.1	Kroenke and Nemoto, 1982	Eldholm and coffin, 2000
Shatsky rise	126–150	2	2.5	Nakanishi et al., 1989	Eldholm and coffin, 2000
Line islands	68–73, 81–86	-	5	Davis et al., 2002	Larson, 1991a
Mid-pacific mountain	117–132	-	22	Smoot, 1999	Larson, 1991a
Caribbean plateau	75, 90	11	4.5	Sinton et al., 1998	Eldholm and coffin, 2000
Caribbean plateau (accreted part)	75, 90	13*	26^+	Sinton et al., 1998	-
Gorgona plateau	75, 90	13*	26^+	Sinton et al., 1998	-
East slawesi ophiolite	138	2.5*	5^+	Parkinson, 1998	-
Iratsu massif	142–153	5*	10^+	e.g., Ozawa et al., 1997	-
Sorachi-Yezo belt	150	8*	16^+	Sakakibara et al., 1997	-
Total		107	191		

* Estimated by assuming oceanic plateau is circle which have the diameter equall to overall length of ophiolite or greenstone belts.
$^+$ Estimated by assuming crustal thickness is 20 km.

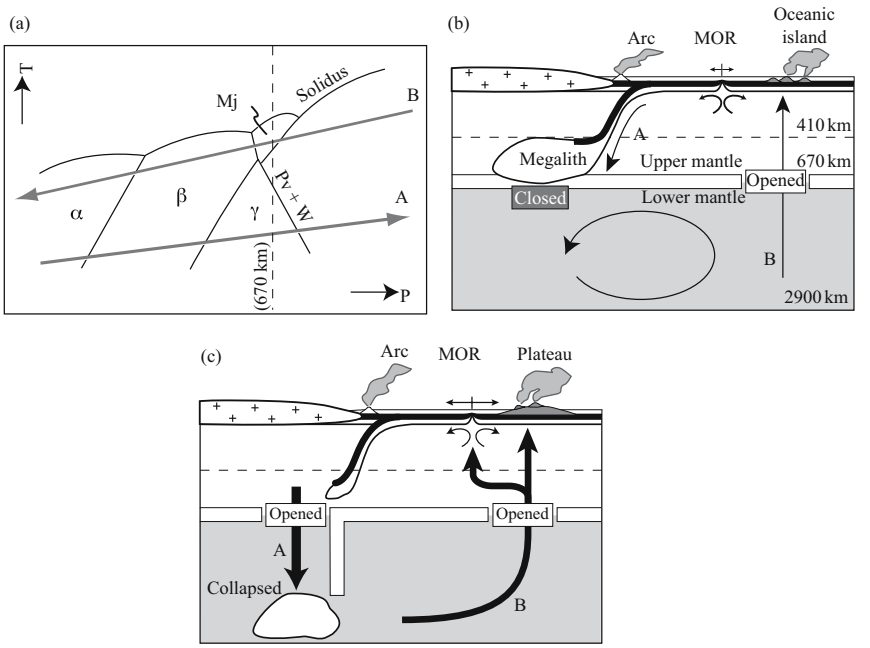


Figure 10. Cartoons showing Cretaceous plate tectonics and a superplume in the Pacific. (a) Schematic phase diagram of mantle peridotite in P-T space (modified after Zhang and Herzberg, 1994; Hirose, 2002) with subduction zone geotherm A and plume geotherm B. The plume geotherm passes the majorite/perovskite transition curve with a positive slope, suggesting that mantle upwelling can be accelerated at ca. 670-km depth to transport fertile lower mantle materials to the upper mantle (See also Kumazawa and Maruyama, 1994). (b) Schematic cross-section showing mantle convection and its related volcanism at a normal stage. (c) Schematic cross-section showing whole-mantle convection and the resultant activated volcanism at a pulse stage. A collapsed megalith accelerates a single-layered convection at a whole-mantle scale.

Hirose, 2002) suggest that a plume geotherm passes the majorite/perovskite transition curve with a positive slope indicating that mantle upwelling can be accelerated at ca. 670-km depth to transport fertile lower mantle materials to the upper mantle (Fig. 10a). Within-plate volcanism related to mantle upwelling indicates that a window between the upper and lower mantle was opened in the Pacific. However, mantle convection at normal times is double-layered and mantle materials are independently circulated within the upper and lower mantles (Fig. 10b). The downwelling beneath a subduction zone due to plate subduction in the circum-Pacific was stopped at 670-km depth by a negative Clausius-Clapeyron slope along the cold geotherm along a subducting plate, resulting in the formation of a megalith (e.g., Irifune and Ringwood, 1993). Subsequently, the megalith collapsed down to the lower mantle, and accelerated a single-layered convection on a whole-mantle scale (Fig. 10c); the resultant mantle upwelling activated episodically. The hot geotherm passes the

majorite/perovskite transition curve with a positive slope, suggesting that mantle upwelling can be accelerated at ca. 670-km depth. As a result, material- and heat-supply from the lower to the upper mantle through the window activated volcanism both at the mid-oceanic ridge and within the plate. The episodic events were not derived from the initiation of a number of plumes (e.g., Richards et al., 1991) but from the pulse of a superplume at a preexisting thermal window.

5 CONCLUSIONS

In summary, the most probable history of the Pacific Ocean and Superplume is as follows. The Pacific Ocean was born by the breakup of the supercontinent Rodinia at ca. 750 Ma. It was derived from the birth of Pacific Superplume. At ca. 550 Ma subduction zones began to develop along the Pacific margin in both eastern Gondwana and western Laurentia. The Pacific Ocean passed through the superocean stage (only one continent and one ocean existed on the earth) from ca. 230 to ca. 180 Ma. These are coincident with the formation of the supercontinent Pangea and the birth of the Atlantic Ocean, respectively. Including circum-Pacific ophiolites and greenstone belts, there were three superplume pulse events (80–150 Ma, 230–300 Ma and 580–600 Ma).

Comparing the Pacific Superplume with the African Superplume, the common relation of a superplume with the surface of the solid earth is as follows. The birth of a superplume arises from the breakup of a supercontinent accompanied by the eruption of continental flood basalts. Prior to this, the formation of a supercontinent occurs in a pre-superplume region. A V-shaped double subduction zone enables the transportation of a vast amount of cold slab into the mantle. This greatly accelerates and creates physical instabilities and chemical heterogeneities in the deep mantle, either or both of which must be deeply concerned with the birth of a superplume. Once a superplume is formed, it behaves as a thermal window. It gives rise to oceanic islands and seamounts in a calm period and oceanic plateaus and oceanic flood basalt in a pulse period.

ACKNOWLEDGEMENTS

Soichi Omori and Kouki Kitajima gave helpful advice that improved our manuscript and Shuji Rino and Shio Watanabe helped draw Figure 1; we express our sincere gratitude to them. This study was supported by a project on Whole Earth Dynamics from the Science and Technology Agency of Japan.

REFERENCES

Acton, G.D., B. Galbun, and J.W. King (2000) Paleolatitude of the Caribbean plate since the Late Cretaceous. *Proc. ODP Sci. Results*, 165, 149–173.

Aitchison, J.C., and T.R. Ireland (1995) Age profile of ophiolitic rocks across the Late Paleozoic New England Orogen, New South Wales: Implications for tectonic models. *Aust. J. Earth Sci.*, 42, 11–23.

Aitchison, J.C., T.R. Ireland, M.C. Blake Jr., and P.G. Flood (1992) 530 Ma age for ophiolite from the New England Orogen: Oldest rocks known from eastern Australia. *Geology*, 20, 125–128.

Baksi, A.K. (1989) Reevaluation of the timing and duration of the extrusion of the Imnaha, Picture Gorge and Grande Ronde Basalts, Columbia River Basalt Group. In Reidel, S.P., and P.R. Hooper (eds.) Volcanism and Tectonism in the Columbia River Flood Basalt Province, Special Paper, vol. 239, Geological Society of America, Boulder, Colorado, US, pp. 105–112.

Baksi, A.K. (1994) Geochronological studies on whole-rock basalts. Deccan Traps, India; evaluation of the timing of volcanism relative to the K-T boundary. *Earth Planet. Sci. Lett.*, 121, 43–56.

Banno, S., and C. Sakai (1989) Geology and metamorphic evolution of the Sanbagawa metamorphic belt, Japan. In Daly, J.S., R.A. Cliff, and B.W.D. Yardley (eds.) Evolution of Metamorphic Belts, Special Publication, vol. 43, Geological Society, London, pp. 519–532.

Barker, F., D.L. Jones, J.R. Budahn, and P.J. Coney (1988) Ocean Plateau-Seamount Origin of Basaltic Rocks, Angayucham Terrane, central Alaska. *J. Geo.*, 96, 368–374.

Black, L.P., D.B. Seymour, K.D. Corbett, S.E. Cox, J.L. Everard, G.R. Green, M.P. McClenaghan, J. Pemberton, D.B. Seymour, J.E. Streit, J. Taheri, and N.J. Turner (1997) *Dating Tasmania's Oldest Geological Events. AGSO Record, 1997/5*.

Boger, S.D., C.J.L. Wilson, and C.M. Fanning (2001) Early Paleozoic tectonism within the East Antarctic craton: The final suture between east and west Gondwana? *Geology*, 29, 463–466.

Brook, F.J., M.J. Isaac, and B.W. Hayward (1988) Geology of autochthonous and allochthonous strata in the Omahua area, northern New Zealand. *New Zealand Geological Survey Record*, 32, 40.

Brouxel, M., and H. Lapierre (1988) Geochemical study of an early Paleozoic island-arc-back-arc basin system. Part 1: The Trinity Ophiolite (northern California). *Geol. Soc. Am. Bull.*, 100, 1111–1119.

Brouxel, M., H. Lapierre, A. Michard, and F. Albalede (1988) Geochemical study of an early Paleozoic island-arc-back-arc basin system. Part 2: Eastern Klamath, early to middle Paleozoic island-arc volcanic rocks (northern California). *Geol. Soc. Am. Bull.*, 100, 1120–1130.

Brouxel, M., C. Lecuyer, and H. Lapierre (1989) Diversity of magma types in a lower Paleozoic island arc-marginal basin system (Eastern Klamath Mountains, California, USA). *Chemical Geology*, 77, 251–264.

Bruce, M.C., Y. Niu, T.A. Harbort, and R.J. Holcombe (2000) Petrological, Geochemical and Geochronological evidence for a Neoproterozoic ocean basin recorded in the Marlborough terrane of the northern New England Fold Belt. *Aust. J. Earth Sci.*, 47, 1053–1064.

Burrett, C., and R. Berry (2000) Proterozoic Australia-western Unites States (AUSWUS) fit between Laurentia and Australia. *Geology*, 28, 103–106.

Buslov, M.M., N.A. Berzin, N.L. Dobretsov, and V.A. Simonov (1993) Geology and Tectonics of Gorny Altai: Guidebook for post-symposium excursion. *The 4th international symposium of the IGCP project 283 Geodynamic evolution of the Paleoasian ocean*, Russian Academy of Sciences, Siberian branch, United Institute of Geology, Geophysics and Mineralogy, Novosibirsk, p. 122.

Buslov, M.M., and T. Watanabe (1996) Intrasubduction collision and its role in the evolution of an accretionary wedge: The Kurai zone of Gorny Altai, Central Asia. *Russian Geol. Geophys.*, 36, 83–94.

Butler, R.F., G.E. Gehrels, and D.R. Bazard (1997) Paleomagnetism of Paleozoic strata of the Alexander terrane, southeastern Alaska. *Geol. Soc. Am. Bull.*, 109, 1372–1388.

Campos Neto, M.C. (2000) Orogenic system from Southwestern Gondwana: An approach to Brasiliano-Pan-African cycle and orogenic collage in southeastern Brazil. In Cordani, U.G., E.J. Milani, A. Thomaz Filho, and D.A. Campos (eds.) Tectonic Evolution of South America, Proceedings of the Thirty-first International Geological Congress, Rio de Janeiro, Brazil, pp. 335–365.

Castillo, P.R., M.S. Pringle, and R.W. Carlson (1994) East Mariana Basin tholeiites: Cretaceous intraplate basalts or rift basalts related to the Ontong Java Plume? *Earth Planet. Sci. Lett.*, 123, 139–154.

Cluzel, D., J.C. Aitchison, and C. Picard (2001) Tectonic accretion and underplating of mafic terranes in the Late Eocene intraoceanic fore-arc of New Caledonia (Southwest Pacific): Geodynamic implications. *Tectonophysics*, 340, 23–59.

Coffin, M.F., and O. Eldholm (1994) Large igneous provinces: Crustal structure, dimensions, and external consequences. *Rev. Geophys.*, 32, 1–36.

Coffin, M.F., and P.D. Rabinowitz (1988) *Evolution of the conjugate East African-Madagascan margins and the western Somali Basin,* Special Paper, vol. 226, p. 78, Geological Society of America, Boulder, Colorado.

Condie, K.C. (2003) Supercontinents, superplumes and continental growth: The Neoproterozoic record. In Yoshida, M., B.F. Windley, and S. Dasgupta (eds.) Proterozoic East Gondwana: Super Continent Assembly and Break-up, Special Publication, vol. 206, Geological Society, London, pp. 1–21.

Courtillot, V., A. Davaille, J. Besse, and J. Stock (2003) Three distinct types of hotspots in the Earth's mantle. *Earth Planet. Sci. Lett.*, 205, 295–308.

Courtillot, V., C. Jaupart, I. Manighetti, P. Tapponnier, and J. Besse (2003) On causal links between flood basalts and continental breakup. *Earth Planet. Sci. Lett.*, 166, 177–195.

Crawford, A.J., and R.F. Berry (1992) Tectonic implications of Late Proterozoic-Early Paleozoic igneous rock associations in western Tasmania. *Tectonophysics*, 214, 37–56.

Crawford, A.J., and R.R. Keays (1987) Petrogenesis of Victorian Cambrian tholeiites and implications for the origin of associated boninites. *J. Petrol.*, 28, 1075–1109.

Dalziel, I.W.D. (1991) Pacific margins of Laurentia and East Antarctica-Australia as a conjugate rift pair: Evidence and implications for an Eocambrian supercontinent. *Geology*, 19, 598–601.

Dalziel, I.W.D. (1992) Antarctica; A tale of two supercontinents? *Annu. Rev. Earth Planet. Sci.*, 20, 501–526.

Dalziel, I.W.D. (1997) Neoproterozoic-Paleozoic geography and tectonics: Review, hypothesis, environmental speculation. *Geol. Soc. Am. Bull.*, 109, 16–42.

Dalziel, I.W.D., L.A. Lawver, and J.B. Murphy (2000) Plumes, orogenesis, and supercontinental fragmentation. *Earth Planet. Sci. Lett.*, 178, 1–11.

Davis, A.S., L.B. Gray, D.A. Clague, and J.R. Hein (2002) The Line Islands revisited: New $^{40}Ar/^{39}Ar$ geochronologic evidence for episodes of volcanism due to lithospheric extension. *Geochem. Geophys. Geosyst.*, 3, doi:10.1029/2001GC000190.

Davis, A., and G. Plafker (1984) Comparative geochemistry and petrology of Triassic basaltic rocks from the Taku terrane on the Chilkat Peninsula and Wrangellia. *Can. J. Earth Sci.*, 22, 183–194.

Davis, J.S., S.M. Roeske, W.C. McClelland, and S.M. Kay (2000) Mafic and ultramafic crustal fragments of the southwestern Precordillera terrane and their bearing on tectonic models of the early Paleozoic in western Argentina. *Geology*, 28, 171–174.

Dobretsov, N.L., M.M. Buslov, and Y. Uchio (2004) Fragments of oceanic islands in accretion–collision areas of Gorny Altai and Salair, southern Siberia, Russia: Early stages of continental crustal growth of the Siberian continent in Vendian–Early Cambrian time. *J. Southeast Asian Earth Sci.*, 23, 673–690.

Dobretsov, N.L., M.M. Buslov, and V.A. Vernikovsky (2003) Neoproterozoic to Early Ordovician evolution of the Paleo-Asian Ocean: Implication to the breakup of Rodinia. *Gondwana Research*, 6, 143–159.

Doig, R., J.B. Murphy, and R.D. Nance (1993) Tectonic significance of the Late Proterozoic Economy River Gneiss, Cobequid Highlands, Avalon composite terrane, Nova Scotia. *Can. J. Earth Sci.*, 30, 474–479.

Duncan, R.A. (2002) A Time frame for construction of the Kergueln Plateau and Broken Ridge. *J. Petrol.*, 43, 1109–1119.

Dziewonski, A.M. (1984) Mapping the lower mantle: Determination of lateral heterogeneity in P velocity up to degree and order 6. *J. Geophys. Res.*, 89, 5929–5952.

Dziewonski, A.M., and J.H.Woodhouse (1987) Global images of the Earth's interior. *Science*, 236, 37–48.

Egal, E., C. Guerrot, D. Le Goff, D. Thieblemont, and J. Chantraine (1996) The Cadomian orogeny revisited in northern France. In Nance, R.D., and M.D. Thompson (eds.) Avalonian and Related Peri-Gondwanan Terranes of the Circum-North Atlantic, Special Paper, vol. 304, Geological Society of America, Boulder, Colorado, pp. 281–318.

Eissen, J.-P., A.J. Crawford, J. Cotten, S. Meffre, H. Bellon, and M. Delaune (1998) Geochemistry and tectonic significance of basalts in the Poya Terrane, New Caledonia. *Tectonophysics*, 284, 203–219.

Eldholm, O., and M.F. Coffin (2000) Large igneous provinces and plate tectonics. In Richards, M.A., R.G. Gordon, and R.D. Van der Hilst (eds.) The History and Dynamics of Global Plate Motions, Geophysical Monograph Series, vol. 121, American Geophysical Union, Washington, D.C., pp. 309–326.

Eldholm, O., and K. Grue (1994) North Atlantic volcanic margins: Dimensions and production rates. *J. Geophys. Res.*, 99, 2955–2968.

Engebretson, D.C., A. Cox, and R.G. Gordon (1985) In Boulder, C.O. (ed.) Relative Motions between Oceanic and Continental Plates in the Pacific Basins, Geological Society of America, Special Paper, 206, p. 59.

Fitzsimons, I.C.W. (2000) Grenville-age basement provinces in East Antarctica: Evidence for three separate collisional orogens. *Geology*, 28, 879–882.

Ford, D., and J. Golonka (2003) Phanerozoic paleogeography, paleoenvironment and lithofacies maps of the circum-Atlantic margins. *Marine and Petroleum Geology*, 20, 249–285.

Frimmel, H.E., R.E. Zartman, and A. Späth (2001) The Richtersveld igneous complex, South Africa: U-Pb zircon and geochemical evidence for the beginning of Neoproterozoic continental breakup. *J. Geol.*, 109, 493–508.

Fukao, Y. (1992) Seismic tomogram of the Earth's mantle: Geodynamic implications. *Science*, 258, 625–630.

Golonka, J., N.Y. Bocharova, D. Ford, M.E. Edrich, J. Bednarczyk, and J. Wildharber (2003) Paleozoic reconstructions and basins development of the Arctic. *Marine and Petroleum Geology*, 20, 211–248.

Gregori, D.G., and E.A. Bjerg (1997) New evidence on the nature of the Frontal Cordillera Ophiolitic Belt—Argentina. *Journal of South American Earth Sciences*, 10, 147–155.

Harlan, S.S., L. Heaman, A.N. LeCheminant, and W.R. Premo (2003) Gunbarrel mafic magmatic event: A key 780 Ma time marker for Rodinia plate reconstructions. *Geology*, 31, 1053–1056.

Gregoire, M., N. Mattieli, C. Nicollet, J.Y. Cottin, H. Leyrit, D. Weis, N. Shimizu, and A. Giret (1994) Oceanic mafic granulite xenoliths from the Kerguelen archipelago. *Nature*, 367, 360–363.

Harper, G.D. (1984) A review of hemipelagic and flysch sedimentation associated with the Josephine ophiolite, California. *Ofioliti*, 19, 397–411.

Heaman, L.M., A.N. LeCheminant, and A.H. Rainbird (1992) Nature and timing of Franklin igneous events, Canada: Implications for a late Proterozoic mantle plume and the break-up of Laurentia. *Earth Planet. Sci. Lett.*, 109, 117–131.

Heinhorst, J., B. Lehmann, P. Ermolov, V. Serykh, and S. Zhurutin (2000) Paleozoic crustal growth and metakkogeny of the Central Asia: Evidence from magmatic-hydrothermal ore system of Central Kazakhstan. *Tectonophysics*, 328, 69–87.

Hervé, F., L. Aguirre, V. Sepulveda, and D. Morata (1999) Contrasting geochemistry and metamorphism of pillow basalts in metamorphic complexes from Aysén, S. Chile. *Journal of South American Earth Sciences*, 12, 379–388.

Herzig, C.T., D.L. Kimbrough, and Y. Hayasaka (1997) Early Permian zircon uranium-lead ages for plagiogranites in the Yakuno ophiolite, Asago distinct, southwest Japan. *The Island Arc*, 6, 396–403.

Hill R.I. (1991) Starting plumes and continental break-up. *Earth Planet. Sci. Lett.*, 104, 398–416.

Hirose, K. (2002) Phase transitions in pyrolitic mantle around 670-km depth: Implications for upwelling of plumes from the lower mantle. *J. Geophys. Res.*, 107, doi:10.1029/2001JB000597.

Hoffman, P.F. (1989) Precambrian geology and tectonic history of North America. In Bally, A.W., and A.R. Palmer (eds.) The Geology of North America-An Overview, Geological Society of America, Boulder, Colorado, USA, pp. 447–512.

Hoffman, P.F. (1991) Did the breakout of Laurentia turn Gondwanaland inside-out? *Science*, 252, 1409–1412.

Hofmann, C., V. Courtillot, G. Féraud, P. Rochette, G.Yirgu, E. Ketefo, and R. Pik (1997) Timing of the Ethiopian flood basalt event and implications for plume birth and global change. *Nature*, 389, 838–841.

Irifune, T., and A.E. Ringwood (1993) Phase relationships in subducted oceanic crust and buoyancy relationships at depths of 600–800 km in the mantle. *Earth Planet. Sci. Lett.*, 117, 101–110.

Ishiwatari, A. (1985a) Igneous petrogenesis of the Yakuno ophiolite (Japan) in the context of the diversity of ophiolites. *Contrib. Mineral. Petrol.*, 89, 155–167.

Ishiwatari, A. (1985b) Granulite-facies metacumulates of the Yakuno ophiolite, Japan: Evidence for unusually thick oceanic crust. *J. Petrol.*, 26, 1–30.

Ishizuka, H., and S. Suzuki (1995) Ophiolite metamorphism and ocean-floor metamorphism. *J. Geog.*, 104, 350–360 (in Japanese with English abstract).

Isozaki, Y. (1997) Contrasting two types of orogen in Permo-Triassic Japan: Accretionary versus collisional. *The Island Arc*, 6, 2–24.

Isozaki, Y., and T. Itaya (1990) Chronology of Sanbagawa metamorphism. *J. Metamo. Geol.*, 8, 401–411.

Isozaki, Y., S. Maruyama, and F. Furuoka (1990) Accreted oceanic materials in Japan. *Tectonophysics*, 181, 179–205.

Jahn, B.-M., W.L. Griffin, and B.F. Windley (eds) (2000) Continental growth in the Phanerozoic: Evidence from Central Asian Orogenic Belt. *Tectonophysics*, 328, 1–227.

Jahn, B.-M., B.F. Windley, B. Natal'in, and N. Dobretsov (eds) (2004) Phanerozoic continental growth in Central Asia. *J. Southeast Asian Earth Sci.*, 23, 599–815.

Johnson, M.C., A.T. Anderson Jr., and M.J. Rutherford (1997) Pre-eruptive volatile contents of magmas. In Carroll, M.R., and J.R. Holloway (eds.) Volatiles in Magmas, Reviews in Mineralogy, vol. 30, Mineralogical Society of America, Washington, D.C., pp. 281–330.

Jones, D.L., N.J. Silberling, and J. Hillhouse (1977) Wrangellia—a displaced terrane in northwestern North America. *Can. J. Earth Sci.*, 14, 2565–2577.

Kadarusman, A., S. Miyashita, S. Maruyama, C.D. Parkinson, and A. Ishikawa (2004) Petrology, geochemistry and paleogeographic reconstruction of the East Sulawesi Ophiolite, Indonesia. *Tectonophysics*, 392, 55–83.

Kamo, S.L., G.K. Czamanske, and T.E. Krogh (1996) A minimum U-Pb age for Siberian flood-basalt volcanism. *Geochim. Cosmochim. Acta*, 60, 3505–3511.

Karlstrom, K.E., K.-I. Åhäll, S. Stephen, S.S. Harlan, M.L. Williams, J. McLelland, and J.W. Geissman (2001) Long-lived (1.8–1.0 Ga) convergent orogen in southern Laurentia, its extensions to Australia and Baltica, and implications for refining Rodinia. *Precambrian Res.*, 111, 5–30.

Karlstrom, K.E., S.S. Harlan, M.L. Williams, J. McLelland, J.W. Geissman, and K.-I. Åhäll (1999) Refining Rodinia: Geologic evidence for the Australian-western US connection in the Proterozoic. *GSA Today*, 9, 1–7.

Kerr, A.C., J.A. Aspden, J. Tarney, and L.F. Pilatasig (2002) The nature and provenance of accreted oceanic terranes in western Ecuador: Geochemical and tectonic constraints. *J. Geol. Soc. London*, 159, 577–594.

Kerr, A.C., G.F. Marriner, N.T. Arndt, J. Tarney, A. Nivia, A.D. Saunders, and R.A. Duncan (1996b) The petrogenesis of Gorgona komatiites, picrites and basalts: New field, petrographic and geochemical constraints. *Lithos*, 37, 245–260.

Kerr, A.C., G.F. Marriner, J. Tarney, A. Nivia, A.D. Saunders, M.F. Thirlwall, and C. Sinton (1997a) Elemental and isotopic constraints on the petrogenesis and original tectonic setting of Cretaceous basaltic terranes in western Colombia. *J. Petrol.*, 38, 667–702.

Kerr, A.C., and J. Tarney (2005) Tectonic evolution of the Caribbean and northwestern South America: The case for accretion of two Late Cretaceous oceanic plateaus. *Geology*, 33, 269–272.

Kerr, A.C., J. Tarney, G.F. Marriner, G.T. Klaver, A.D. Saunders, and M.F. Thirlwall (1996a) The geochemistry and petrogenesis of the late-Cretaceous picrites and basalts of Curacao, Netherlands Antilles: A remnant of an oceanic plateau. *Contrib. Mineral. Petrol.*, 124, 29–43.

Kerr, A.C., J. Tarney, G.F. Marriner, A. Nivia, and A.D. Saunders (1997b) The Caribbean-Colombian Cretaceous Igneous Province: The internal anatomy of an oceanic plateau. In Mahoney, J.J., and M.F. Coffin (eds.) Large Igneous Provinces; Continental, Oceanic, and Planetary Flood Volcanism, Geophysical Monograph Series, vol. 100, American Geophysical Union, Washington, D.C., pp. 123–144.

Kerrick, D.M., and K. Caldeira (1993) Paleoatmospheric consequences of CO_2 released during early Cenozoic regional metamorphism in the Tethyan orogen. *Chem. Geol.*, 108, 201–230.

Khain, E.V., E.V. Bibikova, E.B. Salnilkova, A. Kröner, A.S. Gibsher, A.N. Dienko, K.E. Degtyarev, and A.A. Fedotova (2003) The Paleo-Asian ocean in the Neoproterozoic and early Paleozoic: New geochronologic data and palaeotectonic reconstructions. *Precambrian Res.*, 122, 329–358.

Kimbrough, D.L., J.M. Mattinson, D.S. Coombs, C.A. Landis, and M.R. Johnson (1992) Uranium-lead ages from the Dun Mountain Ophiolite Belt and Brook Street terrane, South Island, New Zealand. *Geol. Soc. Am. Bull.*, 104, 429–443.

Kiminami, K., S. Miyashita, and K. Kawabata (1994) Ridge collision and in-situ greenstones in accretionary complex: An example from the Late Cretaceous Ryukyu Island and southwest Japan margin. *The Island Arc*, 3, 103–111.

Kimura, G., M. Sakakibara, and M. Okamura (1994) Plumes in central Panthalassa? Deductions from accreted oceanic fragments in Japan. *Tectonics*, 13, 905–916.

Kravchinsky, V.A., K.M. Konstantinov, and J.-P. Cogne (2001) Palaeomagnetic study of Vendian and Early Cambrian rocks of South Siberia and Central Mongolia: Was the Siberian platform assembled at this time? *Precambrian Res.*, 110, 61–92.

Kroenke, L.W., and K. Nemoto (1982) Marine geology of the Hess Rise 2. Basement Morphology, Sediment thickness, and structural geology. *J. Geophys. Res.*, 87, 9259–9278.

Kugimiya, Y., and A. Takasu (2002) Geology of the Western Iratsu mass within the tectonic melange zone in the Sambagawa metamorphic belt, Besshi district, central Shikoku, Japan. *J. Geol. Soc. Jpn.*, 108, 644–662 (In Japanese with English abstract).

Kumazawa, M., and S. Maruyama (1994) Whole Earth tectonics. *J. Geol. Soc. Jpn.*, 100, 81–102.

Kuzmichev, A.B., E.V. Bibikova, and D.Z. Zhuravlev (2001) Neoproterozoic (∼800 Ma) orogeny in the Tuva-Mongolia Massif (Siberia): Island arc-continent collision at the northeast Rodinia margin. *Precambrian Res.*, 110, 109–126.

Lanphere, M.A., and G.B. Dalrymple (1976) K-Ar ages of basalts from DSDP Leg33: Sites 315 (Line Islands) and 317 (Manihiki Plateau). *Initial Report of the Deep Sea Drilling Project*, 33, 649–654.

Larson, R.L. (1991a) Latest pulse of Earth: Evidence for a mid-Cretaceous superplume. *Geology*, 19, 547–550.

Larson, R.L. (1991b) Geological consequences of superplumes. *Geology*, 19, 963–966.

Lassiter, J.C., D.J. DePaolo, and J.J. Mahoney (1995) Geochemistry of the Wrangellia Flood Basalt Province: Implications for the role of continental and oceanic lithosphere in flood basalt genesis. *J. Petrol.*, 36, 983–1009.

Li, Z.X. (2000) New palaeomagnetic results from the 'cap dolomite' of the Neoproterozoic Walsh tillite, northwestern Australia. *Precambrian Res.*, 100, 359–370.

Li, Z.X., X.H. Li, P.D. Kinny, and J. Wang (1999) The breakup of Rodinia: Did it start with a mantle plume beneath South China? *Earth Planet. Sci. Lett.*, 173, 171–181.

Li, Z.X., and C.McA. Powell (2001) An outline of the paleogeographic evolution of the Australasian region since the beginning of the Neoproterozoic. *Earth Sci. Rev.*, 53, 237–277.

Lindsley-Griffin, N. (1994) The Cambrian Trinity ophiolite and related rocks of the Lower Paleozoic Trinity complex, northern California, USA. In Ishiwatari, A., J. Malpas, and H. Ishizuka (eds.) Proceedings of the 29th IGC Ophiolite Symposium, Circum-Pacific Ophiolites, VSP International Science Publishers, Netherlands, pp. 47–68.

Liou, J.G., S. Maruyama, X. Wang, and S. Graham (1990) Precambrian blueschist terranes of the world. *Tectonophysics*, 181, 97–111.

Livermore, R., A. Nankivell, G. Eagles, and P. Morris (2005) Paleogene opening of Drake Passage. *Earth Planet. Sci. Lett.*, 236, 459–470.

Lo, C.-H., S.-L. Chung, T.-Y. Lee, and G. Wu (2002) Age of the Emeishan flood magmatism and relations to Permian-Triassic boundary events. *Earth Planet. Sci. lett.*, 198, 449–458.

Lytwyn, J., J. Casey, S. Gilbert, and T. Kusky (1997) Arc-like mid-ocean ridge basalt formed seaward of a trench-forearc system just prior to ridge subduction: An example from subaccreted ophiolites in southern Alaska. *J. Geophys. Res.*, 102, 10225–10243.

MacDonald, W.D., J.J. Estrada, and G. Humberto (1997) Paleoplate affiliations of volcanic accretionary terranes of the northern Andes. *Geological Society of America Abstract with Program*, 29, 245.

MacPherson, G.J., and S.P. Phipps (1988) Geochemistry and petrology of mafic volcanic rocks from olistostromes in the basal Great Valley Group, northern California Coast Ranges. *Geol. Soc. of Am. Bull.*, 100, 1770–1779.

Maher, S., D.H. Moore, A.J. Crawford, R. Twyford, and C.M. Fanning (1997) Test Drilling of the Southern Margin of the Murray Basin. *Victorian Initiative for Minerals and Petroleum Report*, 52, 275.

Mahoney, J.J., M. Storey, R.A. Duncan, K.J. Spencer, and M. Pringle (1993) Geochemistry and geochronology of the Ontong Java Plateau. In Pringle, M., W. Sager, W. Sliter, and S. Stein (eds.) The Mesozoic Pacific. Geology, Tectonics, and Volcanism, Geophysical Monograph Series, vol. 77, American Geophysical Union, Washington, D.C., pp. 233–261.

Malpas, J., I.E.M. Smith, and D. Williams (1994) Comparative genesis and tectonic setting of ophiolitic rocks of the South and North Islands of New Zealand. In Ishiwatari, A., J. Malpas, and H. Ishizuka (eds.) Proceedings of the 29th IGC Ophiolite Symposium, Circum-Pacific Ophiolites, VSP International Science Publishers, Netherlands, pp. 29–46.

Malpas, J., K.B. Spörli, P.M. Black, and I.E.M. Smith (1992) Northland ophiolite, New Zealand, and implications for plate-tectonic evolution of the southwest Pacific. *Geology*, 20, 149–152.

Mann, P., and A. Taira (2004) Global tectonic significance of the Solomon Island and Ontong Java plateau convergent zone. *Tectonophysics*, 389, 137–190.

Marsh, J.S., P.R. Hooper, J. Rehacek, R.A. Duncan, and A.R. Duncan (1997) Stratigraphy and age of Karoo basalts of Lesotho and implications for correlations within the Karoo Igneous Province. In Mahoney, J.J., and M.F. Coffin (eds.) Large Igneous Provinces; Continental, Oceanic, and Planetary Flood Volcanism, Geophysical Monograph Series, vol. 100, American Geophysical Union, Washington, D.C., pp. 247–272.

Maruyama, S. (1994) Plume tectonics. *J. Geol. Soc. Jpn.*, 100, 24–49.

Maruyama, S. (1997) Pacific-type orogeny revised: Miyashiro-type orogeny proposed. *The Island Arc*, 6, 91–120.

Maruyama, S., Y. Kaneko, T. Ota, M. Terabayashi, H. Yamamoto, I. Katayama, K. Okamoto, T. Komiya, H. Ozawa, R. Anma, A. Ishikawa, J.G. Liou, and B.F. Windley (2001) A speculation of Sanbagawa metamorphism; from accretion at trench through deep subduction to the surface exposure. *Abstracts in UHPM Workshop 2001 at Waseda University, Fluid/Slab/Mantle Interactions and Ultrahigh-P Minerals*, Tokyo, 243–246.

Maruyama, S., J.G. Liou, and M. Terabayashi (1996) Blueschists and Eclogites of the World and Their Exhumation. *Internat. Geol. Rev.*, 38, 485–594.

Maruyama, S., and T. Seno (1986) Orogeny and relative plate motions: Example of the Japanese Islands. *Tectonophysics*, 127, 305–329.

Marzoli, A., L. Melluso, V. Morra, P.R. Renne, I. Sgrosso, M. D'Antonio, L. Duarte, E.A.A. Morais, E.A.A. Morais, and G. Ricci (1999a) Geochronology and petrology of cretaceous basaltic magmatism in the Kwanza Basin (western Angola), and relationships with the Paraná-Etendeka flood basalt province. *J. Geodynam.*, 28, 341–356.

Marzoli, A., P.R. Renne, E.M. Piccirillo, M. Ernesto, G. Bellieni, and A. De Min (1999b) Extensive 200 million year old continental flood basalts of the central Atlantic magmatism province. *Science*, 284, 616–618.

Matsuda, T., and Y. Isozaki (1991) Well-documented travel history of Mesozoic pelagic chert, from mid-oceanic ridge to subduction zone. *Tectonics*, 10, 475–499.

McDougall, I., L. Kristjansson, and K. Saemundsson (1984) Magnetostratigraphy and geochronology of NW-Iceland. *J. Geophys. Res.*, 89, 7029–7060.

Meert, J.G. (2003) A synopsis of events related to the assembly of eastern Gondwana. *Tectonophysics*, 362, 1–40.

Montogomery, H., E.A.J. Pessagno, J.F. Lewis, and J. Schellekens (1994) Paleogeography of Jurassic fragments in the Caribbean. *Tectonics*, 13, 725–732.

Moores, E.M. (1991) Southwest US—East Antarctic (SWEAT) connection: A hypothesis. *Geology*, 19, 425–428.

Morgan, W.J. (1981) Hot spot tracks and the opening of the Atlantic and Indian oceans: The oceanic lithosphere. In Emiliani, C. (ed.) The Sea-Ideas and Observations on Progress in the Study of the Seas, vol. 7, Wiley Interscience, New York, pp. 443–487.

Müller, R.D., D. Mihut, and S. Baldwin (1998) A new kinematic model for the formation and evolution of the West and Northwest Australian margin. In Purcell, P.G., and R.R. Purcell (eds.) The Sedimentary Basins of Western Australia, vol. 2, Proceedings of Petroleum Exploration Society of Australia Symposium, Perth, pp. 55–72.

Nagahashi, T., and S. Miyashita, (2002) Petrology of the greenstones of the Lower Sorachi Group in the Sorachi-Yezo Belt, central Hokkaido, Japan, with special reference to discrimination between oceanic plateau basalts and mid-oceanic ridge basalts. *The Island Arc*, 11, 122–141.

Nakanishi, M., W.W. Sager, and A. Klaus (1999) Magnetic lineations within Shatsky Rise, northwest Pacific Ocean: Implication for hot spot-triple junction interaction and oceanic plateau formation. *J. Geophys. Res.*, 104, 7539–7556.

Nakanishi, M., K. Tamaki, and K. Kobayashi (1989) Mesozoic magnetic anomaly lineations and seafloor spreading history of the northwestern Pacific. *J. Geophys. Res.*, 94, 15437–15462.

Nakanishi, M., and E.L. Winterer (1998) Tectonic history of the Pacific-Farallon-Phoenix triple junction from Late Jurassic to Early Cretaceous: An abandoned Mesozoic spreading system in the central Pacific basin. *J. Geophys. Res.*, 103, 12453–12468.

Neal, C.R., J.J. Mahoney, L.W. Kroenke, R.A. Duncan, and M.G. Petterson (1997) The Ontong Java Plateau. In Mahoney, J.J., and M.F. Coffin (eds.) Large Igneous Provinces; Continental, Oceanic, and Planetary Flood Volcanism, Geophysical Monograph Series, vol. 100, American Geophysical Union, Washington, D.C., pp. 183–216.

Nicholson, K.N., P.M. Black, and C. Picard (2000) Geochemistry and tectonic significance of the Tangihua Ophiolite Complex, New Zealand. *Tectonophysics*, 321, 1–15.

Norvick, M.S., and M.A. Smith (2001) Mapping the plate tectonic reconstruction of southern and south-eastern Australia and implications for petroleum systems. *Australian Petroleum Production and Exploration Association Journal*, 41, 15–35.

O'Connor, J.M., and R.A. Duncan (1990) Evolution of the Walvis Ridge-Rio Grande Rise hot spot system: Implications for African and South American plate motions over plumes. *J. Geophys. Res.*, 95, 17475–17502.

Okamoto, K., H. Shinjoe, I. Katayama, K. Terada, Y. Sano, and S. Johnson (2004) SHRIMP U-Pb dating of quartz-bearing eclogite from the Sanbagawa belt, south-west Japan: Implications for metamorphic evolution if subducted protolith. *Terra Nova*, 16, 81–89.

Ozawa, H., S. Motoyama, S. Inoue, Y. Kato, and M. Murata (1999) Petrology of basic volcanics of the Mikabu greenstone complex in the eastern Shikoku. *Mem. Geol. Soc. Jpn.*, 52, 217–228 (in Japanese with English abstract).

Ozawa, H., M. Murata, H. Nishimura, and T. Itaya (1997) Petrological feature and dating of igneous rocks of the Mikabu belt. *Bull. Volcanol. Soc. Jpn.*, 42, S231–237 (in Japanese with English abstract).

Pallister, J.S., J.R. Budahn, and B.L. Murchy (1989) Pillow basalts of the Angayucham Terrane; oceanic plateau and island crust accreted to the Brooks Range. *J. Geophys. Res.*, 94, 15901–15923.

Parkinson, C.D. (1998) Emplacement of the East Sulawesi Ophiolite: Evidence from subophiolite metamorphic rocks. *J. Southeast. Asian Earth Sci.*, 6, 1–16.

Pimentel, M.M., L. Heaman, and R.A. Fuck (1991) U-Pb zircon and sphene geochronology of Late Proterozoic volcanic arc rock units from southwestern Goiás, central Brazil. *Journal of South American Earth Sciences*, 4, 329–339.

Pisarevsky, S.A., M.T.D. Wingate, C.McA. Powell, S. Johnson, and D.A.D. Evans (2003) Models of Rodinia assembly and fragmentation. In Yoshida, M., B.F. Windley, and S. Dasgupta (eds.) Models of Rodinia assembly and fragmentation, Special Publications, vol. 206, Geological Society, London, pp. 35–55.

Powell, C.McA., Z.X. Li, M.W. McElhinny, J.G. Meert, and J.K. Park (1993) Paleomagnetic constraints on timing of the Neoproterozoic breakup of Rodinia and Cambrian formation of Gondwana. *Geology*, 21, 889–892.

Powell, C.McA., and S.A. Pisarevsky (2002) Late Neoproterozoic assembly of East Gondwanaland. *Geology*, 30, 3–6.

Pringle, M.S. (1992) Radiometric ages of basaltic basement recovered at Sites 800, 801 and 802, ODP Leg 129, western Pacific Ocean. *Proc. ODP Sci. Results*, 129, 389–404.

Pringle, M.S., M. Storey, and J. Wijbrans (1994) $^{40}Ar/^{39}Ar$ geochronology of Mid-Cretaceous Indian Ocean basalts: Constraints on the origin of the large flood basalt provinces. EOS Transactions, American Geophysical Union, 75, Fall Meeting Supplement, abstract, p. 728.

Radhakrishna, T., and M. Joseph (1996) Proterozoic paleomagnetism of the mafic dyke swarms in the high-grade region of southern India. *Precambrian Res.*, 76, 31–46.

Ramana, M.V., T. Ramprasad, and M. Desa (2001) Seafloor spreading magnetic anomalies in the Enderby Basin, East Antarctica. *Earth Planet. Sci. Lett.*, 191, 241–255.

Richards, M.A., R.A. Duncan, and V.E. Courtillot (1989) Flood basalts and hot-spot tracks; plume heads and tails. *Science*, 246, 103–107.

Richards, M.A., D.L. Jones, R.A. Duncan, and D.J. Depaolo (1991) A mantle plume initiation model for the Wrangellia Flood Basalt and other oceanic plateau. *Science*, 254, 263–267.

Richardson, W.P., E.A. Okal, and S. Van der Lee (2000) Rayleigh-wave tomography of the Ontong-Java Plateau. *Phys. Earth Planet. Inter.*, 118, 29–51.

Riley, T.R., P.T. Leat, B.C. Storey, I.J. Parkinson, and I.L. Millar (2003) Ultramafic lamprophyres of the Ferrar large igneous province: Evidence for a HIMU mantle component. *Lithos*, 66, 63–76.

Ringwood, A.E. (1975) Composition and Petrology of the Earth's mantle, McGraw-Hill, New York, p. 618.

Rollinson, H. (1993) Using Geochemical Data: Evaluation, Presentation, Interpretation, Longman, UK, p. 352.

Ruffman A., and J.D. Greenough (1990) The Weekend dykes, a newly recognized mafic dyke swarm on the eastern shore of Nova Scotia, Canada. *Can. J. Earth Sci.*, 27, 644–648.

Sakakibara, M., R.S. Hori, G. Kimura, M. Ikeda, T. Moumoto, and H. Kato (1999) The age of magmatism and petrochemical characteristics of the Sorachi plateau reconstructed in Cretaceous accretionary complex, central Hokkaido, Japan. *Mem. Geol. Soc. Jpn.*, 52, 1–15 (in Japanese with English abstract).

Sakakibara, M., R.S. Hori, and T. Murakami (1993) Evidence from the radiolarian chert xenoliths for post-Jurassic volcanism of the Mikabu greenrocks, Okuki area, western Shikoku, Japan. *J. Geol. Soc. Jpn.*, 99, 831–833.

Saleeby, J.B., G.D. Harper, A.W. Snoke, and W.D. Sharp (1982) Time relations and structural-stratigraphic patterns in ophiolite accretion, West Central Klamath Mountains, California. *J. Geophys. Res.*, 87, 3831–3848.

Sano, S., K. Tazaki, Y. Koide, T. Nagao, T. Watanabe, and Y. Kawachi (1997) Geochemistry of dike rocks in Dun Mountain Ophiolite, Nelson, New Zealand. *N.Z. J. Geol. Geophys.*, 40, 127–136.

Saunders, A.D., J.G. Fitton, A.C. Kerr, M.J. Norry, and R.W. Kent (1997) The North Atlantic igneous province. In Mahoney, J.J., and M.F. Coffin (eds.) Large Igneous Provinces; Continental, Oceanic, and Planetary Flood Volcanism, Geophysical Monograph Series, vol. 100, American Geophysical Union, Washington, D.C., pp. 45–93.

Scarrow, J.H., V. Pease, C. Fleutelot, and V. Dushin (2001) The late Neoproterozoic Enganepe ophiolite, Polar Urals, Russia: An extension of the Cadomian arc? *Precambrian Res.*, 110, 255–275.

Scotese, C.R. (2004) A continental drift flipbook. *J. Geol.*, 112, 729–741.

Shervais, J.W., and D.L. Kimbrough (1985) Geochemical evidence for the tectonic setting of the Coast Range ophiolite: A composite island arc- oceanic crust terrane in western California. *Geology*, 13, 35–38.

Shiraishi, K., Y. Motoyoshi, Y. Nakai, D.J. Ellis, Y. Hiroi, and C.M. Fanning (1994) Cambrian orogenic belt in East Antarctica and Sri Lanka: Implications for Gondwana assembly. *J. Geol.*, 102, 47–65.

Sinton, C.W., R.A. Duncan, M. Storey, J. Lewis, and J.J. Estrada (1998) An oceanic flood basalt province within the Caribbean plate. *Earth Planet. Sci. Lett.*, 155, 221–235.

Sivell, W.J. (2002) Geochemistry and Nd-isotope systematics of chemical and terrigenous sediments from the Dun Mountain Ophiolite, New Zealand. *N.Z. J. Geol. & Geophys.*, 45, 427–451.

Sivell, W.J., and M.T. McCulloch (2000) Reassessment of the origin of the Dun Mountain Ophiolite, New Zealand: Nd-isotopic and geochemical evolution of magma suites. *N.Z. J. Geol. & Geophys.*, 43, 133–146.

Smoot, N.C. (1999) Orthogonal intersections of megatrends in the Western Pacific ocean basin: A case study of the Mid-Pacific mountains. *Geomorphology*, 30, 323–356.

Spaggiari, C.V., D.R. Gray, and D.A. Foster (2003) Tethyan- and Cordilleran-type ophiolites of eastern Australia: Implications for the evolution of the Tasmanides. In Dilek, Y., and P.T. Robinson (eds.) Ophiolites in Earth History, Special Publications, vol. 218, Geological Society, London, pp. 517–539.

Stein, M., and S.L. Goldstein (1996) From plume head to continental lithosphere in the Arabian-Nubian shield. *Nature*, 382, 773–778.

Stewart, K., S. Turner, S. Kelley, C.J. Hawkesworth, L. Kirstein, and M.S.M. Mantonavi (1996) 3-D ^{40}Ar-^{39}Ar geochronology in the Palaná flood basalt province. *Earth Planet. Sci. Lett.*, 143, 95–110.

Storey, M., J.J. Mahoney, and A.D. Saunders (1997) Cretaceous basalts in Madagascar and the transition between plume and continental lithosphere mantle source. In Mahoney, J.J., and M.F. Coffin (eds.) Large Igneous Provinces; Continental, Oceanic, and Planetary Flood Volcanism, Geophysical Monograph Series, vol. 100, American Geophysical Union, Washington, D.C., pp. 95–122.

Storey, M., J.J. Mahoney, A.D. Saunders, R.A. Duncan, S.P. Kelley, and M.F. Coffin (1995) Timing of hot-spot related volcanism and the breakup of Madagascar and India. *Science*, 267, 852–855.

Sun, S.-S., and W.F. McDonough (1989) Chemical and isotopic systematics of oceanic basalts; implications for mantle composition and processes. In Saunders A.D., and M.J. Norry (eds.) Magmatism in the Ocean Basins, Special Publication, vol. 42, Geological Society, London, UK, pp. 313–345.

Sun, S.-S., and J.W. Sheraton (1996) Geochemical and isotopic evolution. In Glikson, A.Y., A.J. Stewart, C.G. Ballhaus, G.L. Clarke, E.H.J. Feeken, J.H. Leven, J.W. Sheraton, and S.-S. Sun (eds.) Geology of the western Musgrave Block, central Australia, with particular reference to the mafic-ultramafic Giles Complex, Australian Geological Survey Organization Bulletin, 239, pp. 135–143.

Suzuki, S., and H. Ishizuka (1998) Low-grade metamorphism of the Mikabu and northern Chichibu belts in central Shikoku, SW Japan: Implications for the areal extent of the Sanbagawa low-grade metamorphism. *J. Metamor. Geol.*, 16, 107–116.

Suzuki, N., A. Kadarusman, and S. Maruyama (2000) Gossira continent: A new name of composite volcanoes formed at South Pacific Superplume during the Cretaceous. Eos Transaction, 81, 48, AGU Fall Meeting Supply, Abstract, V62B–33.

Svenningsen, O.M. (2001) Onset of seafloor spreading in the Iapetus ocean at 608 Ma: Precise age of the Sarek Dyke Swarm, northern Swedish Caledonides. *Precambrian Res.*, 110, 241–254.

Tatsumi, Y., H. Shinjoe, H. Ishizuka, W.W. Sager, and A. Klaus (1998) Geochemical evidence for a mid-Cretaceous superplume. *Geology*, 26, 151–154.

Tejada, M.L.G., J.J. Mahoney, R.A. Duncan, and M.P. Hawkins (1996) Age and geochemistry of basement and alkalic rocks of Malaita and Santa Isabel, Solomon Islands, southern margin of Ontong Java Plateau. *J. Petrol.*, 37, 361–369.

Terabayashi, M., K. Okamoto, H. Yamamoto, Y. Kaneko, T. Ota, S. Maruyama, I. Katayama, T. Komiya, A. Ishikawa, R. Anma, H. Ozawa, B.F. Windley, and J.G. Liou (2005) Accretionary complex origin of the mafic-ultramafic bodies of the Sanbagawa belt, Central Shikoku, Japan. *Intl. Geol. Rev.*, 47, 1058–1073.

Thompson, P.M.E., P.D. Kempton, R.V. White, A.C. Kerr, J. Tarney, A.D. Saunders, J.G. Fitton, and A. McBirney (2003) Hf-Nd isotopic constraints on the origin of the Cretaceous Caribbean plateau and its relationship to the Galapagos plume. *Earth Planet. Sci. Lett.*, 217, 59–75.

Tolan, T.L., S.P. Reidel, M.H. Beeson, J.L. Anderson, K.R. Fecht, and D.A. Swanson (1989) Revisions to the estimates of the aerial extent and volume of the Columbia River Basalt Group. In Reidel, S.P., and P.R. Hooper (eds.) Volcanism and Tectonism in the Columbia River Flood Basalt Province, Special Paper, vol. 239, Geological Society of America, Boulder, Colorado, pp. 1–20.

Uchio, Y., Y. Isozaki, T. Ota, A. Utsunomiya, M.M. Buslov, and S. Maruyama (2004) The oldest mid-oceanic carbonate buildup complex: Setting and lithofacies of the Vendian (Late Neoproterozoic) Baratal limestone in the Gorny Altai Mountains, Siberia. *Proc. Jpn. Acad.*, 80(B), 422–428.

Uesugi, J., and S. Arai (1999) The Shiokawa peridotite mass in the Mikabu belt, central Japan, as a cumulate from intra-plate tholeiite. *Mem. Geol. Soc. Jpn.*, 52, 229–242 (in Japanese with English abstract).

Wallin, E.T., J.M. Mattinson, and A.W. Potter (1988) Early Paleozoic magnetic events in the eastern Klamath Mountains, northern California. *Geology*, 16, 144–148.

Weil, A.B., J.W. Geissman, and R. Van der Voo (2004) Paleomagnetism of the Neoproterozoic Chuar Group, Grand Canyon Supergroup, Arizona: Implications for Laurentia's Neoproterozoic APWP and Rodinia break-up. *Precambrian Res.*, 129, 71–92.

Weil, A.B., R. Van der Voo, C.M. Niocaill, and J.G. Meert (1998) The Proterozoic supercontinent Rodinia: Paleomagnetically derived reconstructions for 1100 to 800 Ma. *Earth Planet. Sci. Lett.*, 154, 13–24.

White, R., and D. McKenzie (1989) Magmatism at rift zones: The generation of volcanic continental margins and flood basalts. *J. Geophys. Res.*, 94, 7685–7729.

White, R.V., J. Tarney, A.C. Kerr, A.D. Saunders, P.D. Kempton, M.S. Pringle, and G.T. Klaver (1999) Modification of an oceanic plateau, Aruba, Dutch Caribbean: Implications of the generation of continental crust. *Lithos*, 46, 43–68.

Wilson, M. (1989) Igneous petrogenesis: A global tectonic approach, Chapman and Hall, London, p. 466.

Windley, B.F. (1995) The Evolving Continents 3rd Ed., John Wiley, Chichester, p. 526.

Wingate, M.T.D., I.H. Campbell, W. Compston, and G.M. Gibson (1998) Ion microprobe U-Pb ages for Neoproterozoic-basaltic magmatism in south-central Australia and implications for the breakup of Rodinia. *Precambrian Res.*, 87, 135–159.

Wingate, M.T.D., and J.W. Giddings (2000) Age and paleomagnetism of the Mundine Well dyke swarm, Western Australia: Implications for an Australia-Laurentia connection at 755 Ma. *Precambrian Res.*, 100, 335–357.

Wingate, M.T.G., S.A. Pisarevsly, and D.A.D. Evans (2002) Rodinia connections between Australia and Laurentia: No SWEAT, no AUSWUS? *Terra Nova*, 14, 121–128.

Winterer, E.L., J.I. Ewing, R.G. Douglas, R.D. Jarrard, Y. Lancelot, R.M. Moberly, T.C. Moore, P.H. Roth, and S.O. Schlanger (eds.) (1973) *Leg 17: Honolulu to Hawaii, Initial Report of the Deep Sea Drilling Project*, 17, p. 930.

Woodhouse, J.H., and A.M. Dziewonski (1984) Mapping the upper mantle: Three-dimensional modeling of Earth structure by inversion of seismic waveforms. *J. Geophys. Res.*, 89, 5953–5986.

Wright, J.E., and S.J. Wyld (1986) Significance of xenocrystic Precambrian zircon contained within the southern continuation of the Josephine ophiolite: Devils Elbow ophiolite remnant, Klamath Mountains, northern California. *Geology*, 14, 671–674.

Wu, F.-Y., J.-Q. Lin, S.A. Wide, X.'O. Zhang, and J.-H. Yang (2005) Nature and significance of the Early Cretaceous giant igneous event in eastern China. *Earth Planet. Sci. Lett.*, 233, 103–119.

Wyld, S.J., and J.E. Wright (1988) The Devils Elbow ophiolite remnant and overlying Galice Formation: New constraints on the Middle to Late Jurassic evolution of Klamath Mountains, California. *Geol. Soc. Am. Bull.*, 100, 29–44.

Yang, K., and P.K. Seccombe (1997) Geochemistry of the mafic and ultramafic complexes of the northern Great Serpentinite Belt, New South Wales: Implications for first stage melting. In Ashley, P.M., and P.G. Flood (eds.) Tectonics and Metallogenesis of the New England Orogen, Special Publication, vol. 19, Geological Society of Australia, Sydney, pp. 197–217.

Yokoyama, K. (1980) Nikubuchi peridotite body in the Sanbagawa metamorphic belt; thermal history of the 'Al-pyroxene-rich suite' peridotite body in high pressure metamorphic terrain. *Contrib. Mineral. Petrol.*, 73, 1–13.

Young, G.M. (1992) Late Proterozoic stratigraphy and the Canada-Australia connection. *Geology*, 20, 215–218.

Zhang, J., and C.T. Herzberg (1994) Melting experiments on anhydrous peridotite KLB-1 from 5.0 to 22.5 Gpa. *J. Geophys. Res.*, 99, 17729–17742.

Zhao, D. (2004) Global tomographic images of mantle plumes and subducting slabs: Insight into deep Earth dynamics. *Phys. Earth Planet. Inter.*, 146, 3–34.

Zindler, A., and S.R. Hart (1986) Chemical geodynamics. *Annu. Rev. Earth Planet. Sci.*, 14, 493–571.